POLITECNICO DI MILANO

Scuola Di Ingegneria

Dipartimento di Elettronica, Informazione e Bioingegneria

Osmotic Pressure Characterization of Glycosaminoglycans using Full-Atomistic Molecular Models

Relatore: Dott. Alfonso Gautieri

Correlatore: Prof. Simone Vesentini

Tesi di:

Alejandro Pando

Matr. 820800

Anno Accademico 2013-2014

"*Everything should be made as*
simple as possible, but no simpler."

-Albert Einstein

Table of Contents

List of Figures

List of Tables

Abstract

The osmotic pressure of Chondroitin Sulfate in a simulated physiological environment of articular cartilage is thoroughly examined *in silico* using full atomistic models. The effects of length (4 vs. 8 monomers), sulfation type (0-, 4-, and 6-sulfation) and ionic strength were investigated in order to elucidate the molecular origins of cartilage biomechanical behavior (focusing on osmotic pressure) providing single-atomistic resolution analyses which would not be attainable with experimental techniques. CS chains exhibit plastic deformation behavior under compressive load, therefore osmotic pressure in the ECM is the main contributor balancing external pressures and this study focuses on quantitatively expressing this contribution. Molecular dynamics was used to recreate the physiological environment experienced inside the extracellular matrix of articular cartilage by CS chains and to simulate the forces acting on the full atomistic chains during compression. To this end, a variety of validation techniques, pre-simulation tasks, and comparisons were conducted in order to validate the test methodology. Preliminaries showed excellent matching results when compared with previous well established studies. Six different CS chain systems with varying lengths and sulfation positions arranged in realistic physiological environments underwent simulation under carrying molar concentrations. Sulfation positioning is found to have negligible influence on CS osmotic pressure behavior, attributed to the small distance between the position of 4- and 6- sulfation relative to the intermolecular spacing between the CS chains. However difference between sulfated and unsulfated chains did have a significant influence on the osmotic pressure. Length of chains was also found to have a significant influence on osmotic pressure as was expected. Osmotic pressures are compared to previous well-established studies and experimental data; and methods for further exploration area discussed.

Astratto

La pressione osmotica di condroitin solfato (CS) in un ambiente fisiologico simulato della cartilagine articolare è accuratamente esaminata in silico utilizzando modelli atomistici completi. Gli effetti di lunghezza (4 vs 8 monomeri), tipo solfatazione (0-, 4- e 6-solfatazione) e la forza ionica sono stati studiati al fine di chiarire le origini molecolari della cartilagine comportamento biomeccanico (incentrati sulla pressione osmotica) fornendo singolo-atomistica risoluzione di analisi che non sarebbe raggiungibile con tecniche sperimentali. Catene CS mostrano un comportamento di deformazione plastica sotto carico di compressione, quindi la pressione osmotica in ECM è il principale contributore bilanciare le pressioni esterne e questo studio si concentra su quantitativamente esprimere questo contributo. Dinamica molecolare è stato utilizzato per ricreare l'ambiente fisiologico sperimentato all'interno della matrice extracellulare della cartilagine articolare da catene CS e di simulare le forze che agiscono sulle catene atomistiche completi durante la compressione. A tal fine, una varietà di tecniche di convalida, attività pre-simulazione, e confronti sono stati condotti al fine di validare la metodologia di prova. Preliminari hanno mostrato ottimi risultati corrispondenti rispetto ai precedenti studi ben consolidati. Sei diversi sistemi di catene CS con lunghezze diverse e posizioni solfatazione disposti in ambienti fisiologici realistici sottoposti a simulazione in svolgimento concentrazioni molari. Posizionamento solfatazione si trova ad avere un'influenza trascurabile sul comportamento pressione osmotica CS, attribuito alla piccola distanza tra la posizione di 4- e 6- solfatazione relative alla distanza intermolecolare tra le catene CS. Tuttavia la differenza tra le catene solfati e solforato ha avuto una notevole influenza sulla pressione osmotica. Lunghezza delle catene è stato anche scoperto di avere una notevole influenza sulla pressione osmotica, come ci si aspettava. Pressioni osmotiche sono confrontati con i precedenti studi affermati e dati sperimentali; e metodi per ulteriore zona di esplorazione discussi.

Chapter 1

INTRODUCTION

Cartilage is a resilient bearing flexible connective tissue found in many areas of the body capable of withstanding loads that are several times that of body weight. Unlike bone and other connective tissue, cartilage is avascular because its function significantly differs from all other tissue. The lack of blood vessels is the reason why cartilage does not possess regenerative properties. Cartilage is located at the end of long bones and is a hydrated biomacromolecular fiber composite that enables proper joint lubrication, articulation, loading, and energy dissipation [20]. It provides a protective lining to the ends of contacting bones during movement with little friction, due to synovial fluid [7]. During joint motion, cartilage can withstand compressive strains of 10–40%, while sustaining a complex combination of compressive, shear, and tensile stresses up to 20 MPa [63]. Cartilage has friction coefficients between ~0.0005 and 0.04 in the presence of synovial fluid, which makes it an excellent lubricator to resistance [22]. It is composed of specialized cells called chondrocytes that produce a dense extracellular matrix of aggrecan and type II collagen. The stiffness of a chondrocyte is two to three orders of magnitude less than that of the ECM, thus these cells do not contribute significantly to the bulk mechanical properties of the tissue [29] Instead the load-bearing capability of cartilage is sustained primarily by two ECM components: the fibrillar collagen network and the highly negatively charged proteoglycan aggrecan.

1.1 Aim of the work

To understand the function of cartilage at the tissue level, cartilage mechanical properties have been studied in detail via many different macroscopic loading configurations, e.g., confined and unconfined compression, pure and simple shear, osmotic swelling, and indentation. The specific objective of this experiment is to conduct an *in silico*, cost-effective evaluation of nanoscale compressive properties of Chondroitin Sulfate (CS) chains at physiological conditions, in order to elucidate the molecular origins

of cartilage biomechanical behavior providing single-atom resolution which otherwise would not be attainable with experimental techniques. This will allows us to attain theoretical insights on cartilage tissue mechanical behavior and Glycosaminoglycan (GAG) characteristics. Toward this end, we develop a physiological system that replicates the environment that CS chains experience in articular cartilage under joint motion for chondroitin sulfate, chondroitin-4-sulfate, and chondroitin-6-sulfate.

1.2 Cartilage

1.2.1 Articular Cartilage at the Molecular level

Cartilage is divided into three different types called hyaline cartilage, fibro cartilage, and elastic cartilage. All three are essential to human function and movement, but hyaline cartilage (also known as articular cartilage) is the most abundant and the one found at the end of long bones. Figure 1.1 below represents the microsystem of articular cartilage which is the principle cartilage this study focuses on. Articular cartilage is found on many freely movable synovial joint surfaces such as the knee and hip [29]. It is a highly specialized connective tissue of diarthrodial joints. It provides absorption, lubrication, and distributes compressive load while withstanding shear stress during joint movement. Most importantly, articular cartilage has a limited capacity for intrinsic healing and repair [29]. Therefore age and certain diseases have a significant impact on cartilage mechanics. Cartilage consists of one cell type known as articular chondrocytes, and the extracellular matrix provided by these cells which can be seen in Figure 1.1. The ECM is principally composed of water, collagen, and proteoglycans, with other noncollagenous proteins and glycoproteins are present in lesser amounts [11].

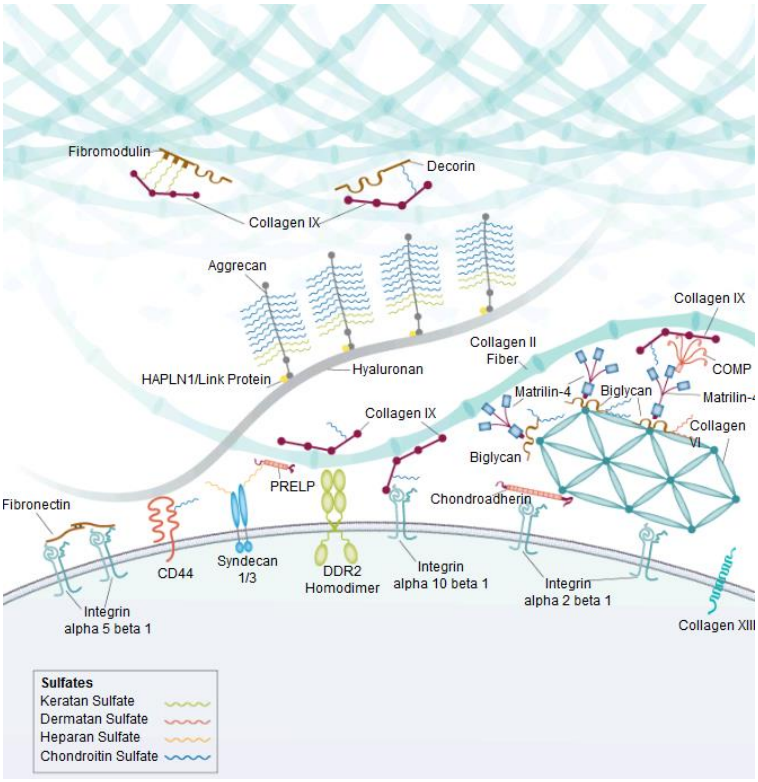

Figure 1.1: The illustration above shows the contents within the extracellular matrix of articular cartilage [3].

Articular cartilage is comprised of four zones known as the superficial zone, the middle zone, the deep zone, and the calcified zone [61]. The superficial zone protects the other layers from shear stress. The collagen fibers of this zone are packed tightly and aligned parallel to the articular surface. The superficial layer plays an important role during joint motion because it is imperative in the stability and maintenance of the deeper layers [63]. This is the zone that has contact with the synovial fluid and exhibits the greatest tensile properties enabling it to withstand sheer, tensile, and compressive forces. After this zone comes the transitional zone, which provides an anatomic and functional bridge between the superficial and deep zone. This zone involves a transition between the shearing forces of surface layer to compression forces in the cartilage layer. It is composed almost entirely of proteoglycans, thus making it the first line of resistance to compressive forces. The deep zone is responsible for providing the greatest resistance to compressive forces, given that collagen fibrils are arranged perpendicular to the articular surface. It is the largest part of the articular cartilage which distributes loads and resists compression. From Figure 1.2, we can see that a tide mark separates the deep zone from the calcified cartilage. The deep zone is responsible for providing the greatest amount of resistance to compressive

forces because it has the highest number of proteoglycans in cartilage. The calcified layer plays an integral role in securing the cartilage to bone, by anchoring the collagen fibrils of the deep zone to the subchondral bone [61].

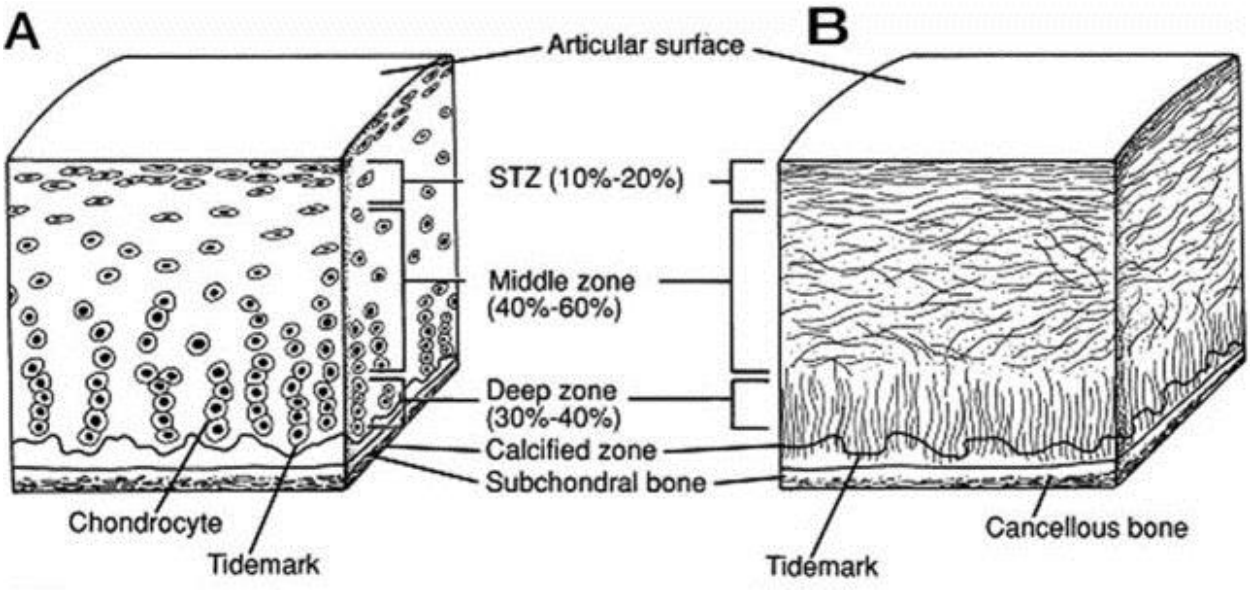

Figure 1.2: Schematic of healthy articular cartilage and all its zones and architecture [12].

1.2.1.1 Extracellular Matrix

The ECM can be divided into three regions based on composition, collagen fibril diameter, and function. The three regions are known as the pericellular, territorial, and interterritorial regions. The pericellular matrix is a thin layer adjacent to the cell membrane that completely surrounds the chondrocyte. It contains mainly proteoglycans and other noncollagenous proteins [61]. This region plays an important role in movement because it initiates the signal transduction within cartilage due to load bearing. The territorial region protects the cartilage cells against the mechanical stresses and contributes to the resilience of the articular cartilage structure to withstand loading. The interterritorial region is the largest of the matrix regions and is characterized by random oriented bundles of large collagen fibrils [20].

In order to understand cartilage at a more detailed level it is important to understand what happens to cartilage at the molecular level and its function under flexion and extension. The cartilage extracellular matrix is a complex of macromolecules. The macromolecules of the cartilage matrix consist of collagen (predominantly type II fibrils), proteoglycan aggregates containing glycosaminoglycan chains, and

multiadhesive glycoproteins (noncollagenous proteins). The most abundant proteoglycan in the cartilage matrix is aggrecan. It is highly negatively charged, brush-like proteoglycan macromolecules that can be expressed in multiple isoforms due to alternative splicing [29]. Aggrecan is the most abundant proteoglycan in cartilage comprising 30–35% of dry tissue weight and has a densely-packed array of highly negatively charged chondroitin sulfate glycosaminoglycan chains along its core protein and is critical to cartilage mechanical function [28]. Its core protein is composed of three globular structural domains (G1, G2, and G3) which are separated by a large extended domain (CS) between G2 and G3 for GAG attachment [36]. G3 makes up the carboxyl term of the core protein. The two main modifier moieties are arranged into distinct regions, a chondroitin sulfate and a keratan sulfate region. Aggrecan is composed of approximately 300 kDa core protein substituted with >100 chondroitin sulfate (CS) and, in some species, keratan sulfate (KS) glycosaminoglycan (GAG) chains [47]. (Figure 1.3)

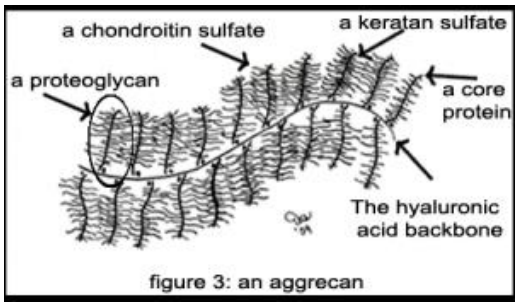

Figure 1.3: Basic model of aggrecan showing the area in question in regards to CS [26]

1.2.1.2 Aggrecan

Aggrecan molecules are bound noncovalently to hyaluronan also known as hyaluronic acid. This binding is stabilized by a small globular protein known as a link protein that is synthesized by chondrocytes independently, and simultaneously with aggrecan and HA [30]. The link protein allows aggrecan to associate noncovalently with high-molecular-weight hyaluronic acid in order to form supramolecular complexes [7]. A single aggrecan molecule contains chondroitin sulfate chains that are covalently bound, at extremely high densities (2-4 nm molecular separation distance), to a 250 KDa protein core [59]. Chondroitin sulfate is a crucial part of the cartilage component and provides much of the resistance to compression and other forces. The tightly packed and highly charged sulfate groups of chondroitin sulfate generate electrostatic repulsion that provides much of the resistance of cartilage to compression. In the early stages of osteoarthritis, aggrecan is one of the first components to be degraded and released from cartilage due to increases in the concentration and activity of enzymes termed aggrecanases. Age, degenerative diseases, and trauma are the major degrading factors of cartilage, because of the degrading effects on chondroitin sulfate. Aggrecanases cleave the covalent links along the core protein amino acid sequence and break aggrecan into smaller fragments, which then diffuse out of the cartilage. The resulting degradation and loss of aggrecan causes instantaneous changes in cartilage biomechanical function, including stiffness and a decrease in load-bearing capacity. These changes lead to further damage by other methods upon continuous joint loading [30].

The biomechanics of cartilage are further explained in order to gain further knowledge of the function of cartilage. Poroelasticity entails a porous media whose solid matrix is elastic and fluid is viscous. A porous material is a solid permeated by an interconnected network of pores filled with a fluid. Poroelasticity can manifest itself in a fluid-solid frictional dissipation and intra-tissue fluid pressurization. These aspects of poroelasticity are essential to mechanical functions of cartilage especially solute and fluid transport, frequency-dependent self-stiffening, load-bearing, energy dissipation, lubrication, and mechanotransduction. AFM based oscillatory compression has been used in studies to measure and predict the frequency-dependent mechanical behavior of superficial zone cartilage [23]. Cartilage ECM is composed mainly of two components defining its mechano-physical properties: the collagenous network, responsible for the tensile strength of the cartilage matrix, and the proteoglycans (mainly aggrecan), responsible for the osmotic swelling and the elastic properties of the cartilage tissue. [29]

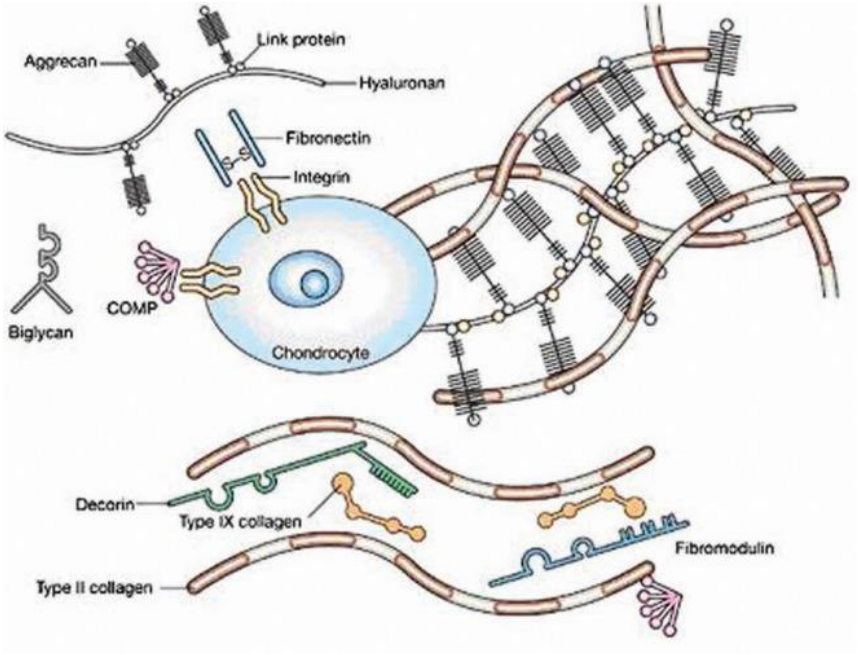

Figure 1.4: The figure above represents the extracellular matrix of articular cartilage. The major load bearing macromolecules are collagens and proteoglycans mainly in aggrecan. The interaction between the highly negatively charged cartilage proteoglycans and type II collagen provides the compressive and tensile strength of the tissue [14].

1.2.1.3 Chondroitin Sulfate

The chondroitin sulfate glycosaminoglycan (CS-GAG) chains of the aggrecan within the ECM, are the major determinant of the tissue's ability to resist compressive loading in vivo. Studies have shown that these compounds are responsible for >50% of the equilibrium compressive elastic modulus under normal physiological conditions (0.15 M salt concentration). They also play a vital role as cell surface receptors and co-receptors, because they mediate behaviors such as recognition, binding and cell to cell signaling [8]. The Chondroitin structure and pattern on aggrecan varies in chemical composition depending on the state of health or disease of articular cartilage which can be severely altered due to age, diseases and other factors. For example, chondroitin-6-sulfate disaccharides show an increase in the human femoral condyle cartilage from birth to the age of 20 years with a concomitant decrease in

chondroitin-4-sulfate after twenty years of age. This aspect is crucial in determining its compressive mechanical properties [59]. The metabolic activity of cartilage cells in the cartilage matric gradually decreases with age; hence the extracellular matrix also changes with age. Studies have shown that more 4-sulfated disaccharides are present in older specimens than in younger ones, while 6-sulfated chondroitin sulfate had the reverse effect. From ages 22 to 65 there are approximately 5 times more C6S than C4S glycosaminoglycans in articular cartilage [8, 59]. These results can be attributed to differences in joint tissue turnover or the cartilage mass persisting in the joint. Studies have also shown that as age increases the ratio of C6S to C4S decreases significantly, while the overall glycosaminoglycan population also decreases within the ECM. This ratio may provide useful information about the happenings within articular cartilage. There has also been evidence that gender plays a role in the metabolism of cartilage. It was recently found that the C6S to C4S ratio was significantly lower in women than in men.

Chondroitin sulfate chains (Figure 1.5) are negatively charged, linear polyelectrolytes composed of between 10 and 50 repeats of the disaccharide (N-acetyl-galactosamine and glucuronic acid) which are extensively substituted with sulfate esters at carbons 4 or 6 of the hexosamine residues. As part of the aggrecan macromolecule, individual CS-GAGs have the tendency to assume an extended, rodlike conformation rather than a random coil under normal physiological conditions of 0.15 M salt concentration due to intramolecular electrostatic repulsion between neighboring negatively charged carboxylate and sulfate groups. The high chain packing density of CS along with its sulfation derivatives play a critical role in determining the mechanical properties of articular cartilage, therefore it is of significant interest to understand the connection between CS composition and its osmotic pressure. [59] Chondroitin sulfate glycosaminoglycans play an important role in compression because they absorb the compressive load exerted on the body [64]. Compression analysis have shown that chondroitin sulfate samples exhibit plastic deformation behavior, therefore these GAG's play a vital role in the compression within articular cartilage.

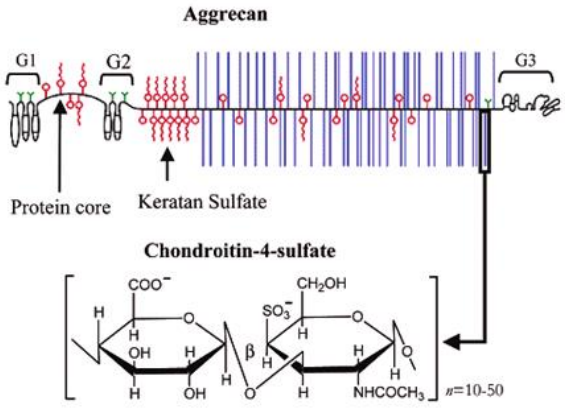

Figure 1.5: An aggrecan core protein containing three globular domains (G1, G2, G3), the CS-GAG attachment region is made of a variable of a chondroitin sulfate region distinguished by their sequence patterns. The second figure shows the chemical structure of the disaccharide repeating unit in chondroitin-4-sulfate glycosaminoglycan [11].

1.3 Biomechanics of Joint Movement

Now that the essential microanatomy of cartilage has been explained, it is important to delve into biomechanical function of joint movement. Articular cartilage has unique viscoelastic properties that provide a smooth, lubricated surface for low friction articulation and facilitate the transmission of loads to the underlying subchondral bone. The biomechanical behavior of articular cartilage will be represented in a biphasic method; a fluid phase and a solid phase. The initial and rapid application of articular contact forces during joint loading causes an immediate increase in the interstitial fluid pressure [42]. This increase in pressure causes the fluid, which is composed of 80 percent water, inorganic ions such as calcium, chloride, sodium, and potassium; to flow out of the ECM, generating a frictional drag on the matrix. The low permeability of cartilage prevents fluid from escaping the matrix as it is compressed. The two opposing bones and surrounding cartilage confine the cartilage under the contact surface. These boundaries are designed to restrict mechanical deformation while providing enough functionality for cartilage to not cause pain in the area [66].

The viscoelastic properties of articular cartilage cause it to exhibit time-dependent behavior when subjected to constant load, which means that part of the energy imparted to the tissue during loading gets dissipated into heat. Therefore when the tissue is unloaded it can restore only the remaining part of the energy imparted to it. The mechanisms responsible for these behaviors are known as flow-

dependent and flow-independent. Since the interstitial fluid of articular cartilage pressurizes under loading, it flows through the tissue's porous collagenous matrix, and the frictional interaction between the fluid and solid constituents contributes significantly to this energy dissipation. This mechanism is described as *flow-dependent* viscoelasticity. *Flow-independent* viscoelasticity occurs when the stored energy dissipates within the solid matrix of the cartilage due to formation and breaking of temporary bonds between the matrix molecules [25]. These mechanisms contribute to stiffening cartilage under dynamic loading conditions. They are caused by macromolecular motion specifically the intrinsic viscoelastic behavior of the collagen-proteoglycan matrix. The fluid pressure provides a significant component of total load support, reducing the stress acting upon the solid matrix.

Articular cartilage also exhibits creep and stress-relaxation behavior, and a hysteric response under loading and unloading. Under a constant compressive force, deformation will increase with time and it will deform or creep until equilibrium has been reached. When cartilage is deformed and held at a constant strain, the stress will rise to a peak, which will be followed by a slow stress-relaxation process until an equilibrium value is reached. [43] Theoretical studies have shown that flow-dependent viscoelastic manifests itself more significantly during compressive loading. [13]. However, when subjected to uniaxial tensile loading, the interstitial fluid pressurization of cartilage would be negligible due to tension-compression nonlinearity; thus it would not contribute to flow-dependent viscoelasticity under this particular loading configuration.

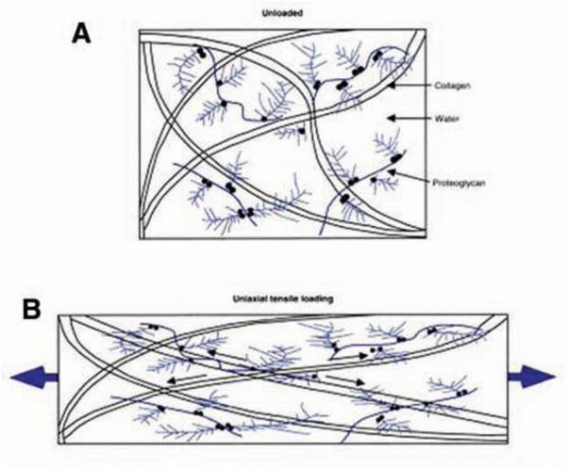

Figure 1.6: A depiction of the extracellular matrix when the tissue is under uniaxial Tensile load and when it is at an unloaded state (B and A, respectively) [50].

Tensile force resisting properties derive from the precise molecular arrangement of collagen fibrils. The stabilization and ultimate tensile strength of the collagen fiber are thought to result from intra and intermolecular cross-links. From Figure 1.6, one can see that the fibrils align along the axis of tension which is in accordance with a stress vs strain graph. Studies have shown that flow-dependent and flow-independent viscoelasticity of cartilage play a critical role in the stiffening of articular layers under dynamic loading, thereby producing relatively small strains despite the large joint loads [50, 13].

The relationship between proteoglycan aggregates and interstitial fluid provides compressive resilience to cartilage through negative electrostatic repulsion forces [13]. Their negatively charged glycosaminoglycan chains interact with electrolytes in the interstitial fluid to produce a Donnan osmotic pressure relative to the external bathing solution of the tissue. This internal pressure swells the tissue and contributes to resisting compressive loads on cartilage.

It is also of primary interest to gain a comprehensive understanding of the molecular origin of the mechanical properties of GAGs and proteoglycans due to their important role in tissue engineering and biomaterial applications. The understanding of the connection between the CS chains and the osmotic pressure is of great importance in order to restore mechanical and biochemical function to cartilage that has been weakened. In order to reach this goal one must analyze the CS chains and their mechanical properties in relation to physiological conditions.

The model uses an all-atom representation of the disaccharide building blocks of GAGs to achieve computational tractability that enables the simulation of physiologically relevant system sizes while retaining the underlying chemical identity of the sugars. In this study we will model chondroitin (CH), chondroitin 4-sulfate (C4S), and chondroitin 6-sulfate (C6S). We will demonstrate theoretically that the model is also directly applicable to the computation of GAG osmotic pressure, and we use it to investigate mechanistically the CS chemical composition osmotic pressure relationship.

1.4 Osmotic Pressure

To maintain an electrically neutral environment within the tissue, an unbalanced distribution of ions will exist and contribute to a net osmotic pressure in the tissue. This pressure causes cartilage to swell acting as a pre-stress and enhances the tissue's ability to bear load. In the past, studies have shown that this pressure ranges from 0.02 to 2.0 MPa [4, 39]. The osmotic modulus is the contribution of osmotic pressure to the compressive stiffness of cartilage, and derives from the rate of this pressure with

compressive strain [4]. The osmotic pressure is directly dependent upon the fixed charge density of its proteoglycans and because the relationship between fixed charge density and compressive strain is given from kinematic considerations, it is possible to estimate the osmotic pressure. The equilibrium osmotic pressure of concentrated glycosaminoglycan's solutions is comprised of both electrostatic and nonelectrostatic contributions. From Donnan law it is known that the electrostatic contribution to the osmotic pressure is dependent on electrolyte concentration, Sodium ions. At high ion concentrations, the presence of excess ions in the solution acts as a shield for the electrostatic repulsion of GAG chains, thus resulting in a decrease of the osmotic pressure of Donnan theory toward zero as the ion concentration increases towards infinity. It is reasonable to conclude, as also reported in previous studies by Ehlrich et al. that the Donnan charge contribution becomes negligible at high concentrations. Chondroitin sulfate 6 comprises about 93.3% of the overall CS in articular cartilage [39].

Chapter 2

MATERIALS AND METHODS

Introduction

This study is composed of a variety of individual steps that together accomplish the task of obtaining the osmotic pressure for GAG chains. To this end, a practical method for accurately computing the osmotic pressure using molecular dynamics was created. Essentially, a system composed of identical CS chains spaced 2 nm apart in an ionized solvated box was made in order to replicate the physiological environment inside articular cartilage. The molar concentrations of the environment was varied in order to account for age, disease and other underlying factors that may possibly influence the character of the articular cartilage matrix. A perpendicular force was exerted on the chains, while allowing the water molecules and ions to freely move in order to gain insight into the characteristics of the GAG chains. The mean force per unit area exerted on the chains by the semipermeable forces can be directly related to the osmotic pressure and is further explained below. Molecular dynamics is the First we will give information about the molecular dynamics theory that underlies all of the modeling and simulations conducted. Then we will proceed to give a detailed description of the theory behind CS chain creation and GAG system construction in physiological environments. Then preliminary tests on the scripts and fundamental ideas conducted in order to validate our work will be discussed along with detailed explanations on our parameters and semipermeable membrane. Finally this thesis will discuss the methods used to generate the osmotic pressure and all it encompasses.

2.1 Mechanical Characterization of Chondroitin Sulfate

Chondroitin sulfate is a sulfated glycosaminoglycan composed of a chain of alternating sugars (N-acetylgalactosamine and glucuronic acid). A typical Chondroitin chain has over a hundred individual sugars each of which can be sulfated in variable positions and quantities [35]. It consists of alternating

disaccharide units of glucuronic acid and galactosamine and is attached to serine residues of the protein cores via a tetrasaccharide linkage. Chondroitin sulfate is an important structural component of cartilage and provides much of its resistance to compression [59]. It is a major component of articular cartilage extracellular matrix, and is important in maintaining the structural integrity of the tissue.

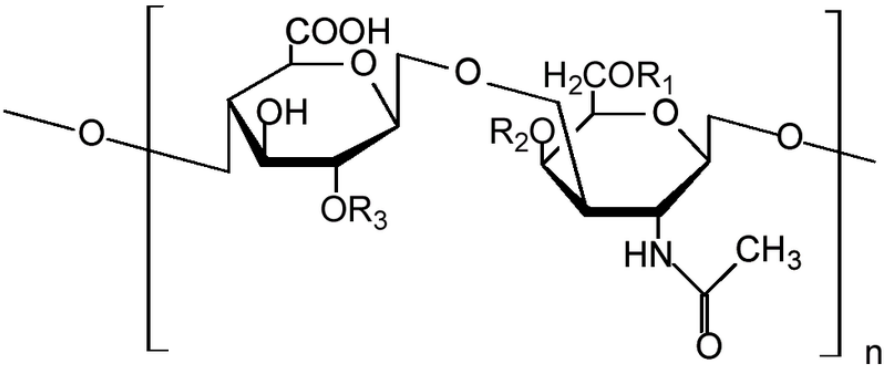

Figure 2.1: One unit structure of a chondroitin sulfate chain [15].

The different chondroitin sulfate chains used in this experiment are comprised of sulfation in different positions of the chains including on the carbon 4 and carbon 6. These specific sulfations were used in order to replicate the conditions experienced in the cartilage. The chondroitin sulfate system is composed of four chains that mimic the physiological environment seen within the extracellular matrix of cartilage. It is important to understand the components that make up glycosaminoglycan chains and the logic behind chondroitin sulfate creation. GAG's are polymers composed of repeating units of disaccharides. Figure 2.1 shown above is an example of a CS disaccharide. CS has been identified as the major sulfated GAG in the matrix of joint tissues and is characterized by repetitive sulfated disaccharide units, β-d-glucuronic acid (GlcUA) and 2-acetamido-2-deoxy-β-d-acetylgalactose (GalNAc), joined by β *(*1⟶4*)* and β *(*1⟶3*)* linkages. Computational modeling has allowed the investigation of this compound at a complex subatomic molecular model but this study takes into account a full atomistic model [17, 15, 59].

In this study, the chondroitin sulfate chains rely on the parameters published by Clipa G et al, who combined the use of experimental techniques and methods of Quantum mechanics to estimate the individual values of C6S disaccharides [17]. The conformations around the glycosidic linkages are described by two sets of torsional angles ψ/ϕ.

The molecular dynamic simulations used in the present study are based on the classical mechanics theory, neglecting all the quantum mechanics effects in order to save computational cost. The equation that represents that state of motion of the molecular system is obtained from the Newtonian equations of motion:

$$m_i * \frac{\partial^2 r_i}{\partial t^2} = F_i$$

Where $F_{i} = -\frac{\partial V}{\partial r_i}$

These relationships allow one to determine the range of movement of a molecular system in relation to that given function. Before the real simulation results were acquired, the system has to be equilibrated for both temperature and pressure stability. During the simulation, temperature undergoes slight oscillations around the set point in order to stabilize and allow for atom control within the parameters specified [10].

2.2 Molecular Dynamics

Molecular Dynamics (MD) is one of the principal computational techniques that allow one to simulate the time dependent behavior of atoms and molecular systems. This method is widely used to investigate mechanical properties at the microscopic level of several molecular and atomistic structures as it can easily study complex systems. The molecular dynamics process is explained in detail in Appendix A.

Molecular simulations are used because they provide better information than in vivo studies for a far less cost in less time. The main survey techniques for Chondroitin Sulfate characterization and properties are Nuclear Magnetic Resonance and X-ray crystallography. Although these methods are beneficial and provide valuable information, they provide only partial information compared with the *in silico* simulations [9]. This is because GAG's do not exhibit a strictly stable confirmation but instead have multiple structures. X-ray crystallography is able to provide general information about the conformational energy distributed throughout the GAG's but the non physiological conditions and the crystalline packaging causes limitations in this method.

Molecular modeling simulations have shown in the past that they have relatively similar results to experimental techniques such as NMR spectroscopy and x-ray crystallography [9, 10]. The molecular modeling techniques for the displacement fields of a system of atoms, relies on the laws of mechanics [10]. This method does not take into account the electron movement throughout the simulation; therefore another method using quantum mechanics would be ideal to get more precise results. This method is the most precise and accurate method on MD simulations but it can only be applied to systems with smaller atoms. Our system is quite large therefore only classical mechanics is used allowing for computational efficiency while remaining precise.

The model developed in this project is similar to previously developed models for polysaccharides including pullulan, xythan, cellulose, laminaran, and CS itself. The differences are that in these models, we want a full atomistic model and not a coarse grained model as those projects had done, along with different parameters for distance and concentration. Most of these studies focused on isolated disaccharides used to generate pretabulated potentials of mean force for the glycosidic torsions which is used to calculate the specific polysaccharide properties corresponding to the unperturbed θ state. Although Bathe's model uses a coarse grained model that includes electrostatic interactions between nonbonded monosaccharides, it does not give the GAGs enough freedom to act as if they were in a physiological environment [10]. In the present work, hydrophobic and Van der Waals interactions are not ignored but are truncated and the script is written so that it focuses on the perceived range of the forces. The sulfations at carbon 4 and carbon 6 are also taken into consideration in this study, providing a precision that before was not possible.

The current study assumes that the conformational energy of the GAG torsion angles is independent from their successors. This implies that hydrogen bonding occurs only across single glycosidic linkages. However, neighboring torsion angles are usually highly interdependent and were treated as such.

2.2.1 Potential Energy Function

The most computationally demanding part of molecular dynamics is the evaluating the forces. The force is the negative gradient of a scalar potential energy function,

$$\vec{F}(\vec{r}) = -\nabla U(\vec{r}),$$

For our study and any system of biomolecules the function below is used:

$$U(\vec{r}) = \sum U_{\text{bonded}}(\vec{r}) + \sum U_{\text{nonbonded}}(\vec{r}),$$

To understand the dynamics of a chemical system we need to understand all the forces operating within the system, hence we need to know the potential surface, U(r). The potential energy surface (PES) is a theoretical concept whose main use lies in the energy description of a system, normally the position of atoms. Since electrons are much lighter than nuclei, they move much faster and adjust adiabatically to any charge in the nuclear configuration. The PES is comprised of the sum of the binding and non-binding terms [21]. To further understand the concept of PSE, the diatomic potential energy curve below is shown (Figure 2.3).

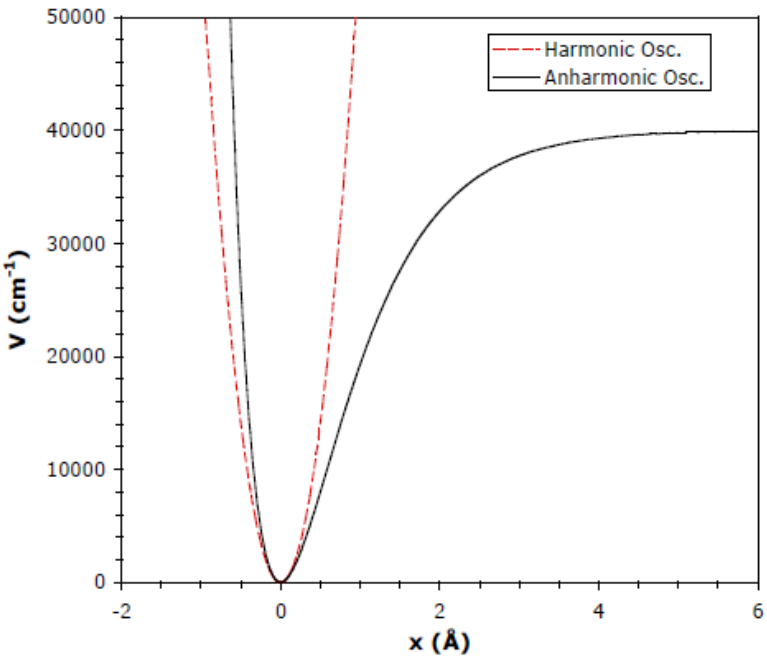

Figure 2.2: The figure shows the relationship between bond energy and bond length; focusing on the differences that arise when comparing the harmonic oscillator (red curve) and the Morse oscillator (black curve). The dissociation energy is visible to the right [32].

The graph represents two potential energy functions for a molecule model. As one can see, the Harmonic oscillator is a more idealistic function, while the Morse oscillator function gives a more accurate and realistic description of the potential energy. The harmonic oscillator potential represents a model for vibrational motion of molecules. The atoms were attached by a single bond that has the same characteristics of a spring. Therefore we assume that a pair of atoms is connected by a spring and is composed of two parameters: an equilibrium distance (r_e) and bond stiffness (k). The form of the potential energy for the harmonic oscillator is:

$$V(x) = \frac{1}{2}kx^2,$$

In the harmonic oscillator, a pair of atoms is considered to have a relationship if there is energy being provided. On the contrary, the Morse oscillator descrambles this misrepresentation, and the potential level spacing decreases as the energy approaches the dissociation energy, which indicates the energy needed to break a bond [40]. The harmonic oscillator model is particularly useful for low vibrational energies but when the energies are high it is preferable to use the Morse oscillator potential which can be seen below:

$$V(x) = D_e\left[1 - e^{-ax}\right]^2$$

The force fields contain the form and parameters of mathematical functions used to describe the potential energy of a system of particles and characterizes the molecular system behavior. Force fields when relating to atomistic and molecular particles can be divided into Reactive Force Fields (RFFs) and Non-Reactive Force Fields (NRFFs). Traditional force fields are unable to model chemical reactions because of the requirement of breaking and forming bonds (a force field's functional form depends on having all bonds defined explicitly) but reactive force fields aim to be as general as possible and have been parameterized and tested for hydrocarbon reactions, transition-metal-catalyzed nanotube formation, and high-energy materials [49]. In the present work, NRFF's are used in order to mimic the physiological properties experienced by CS chains inside articular cartilage. NRFFs simulate bond interaction as harmonic springs and bonds cannot be created or broken because as the distance between two atoms increases the energy increases as well.

2.2.2 Dihedral Angles

For bonded potential energy the 4-body torsion angle known as dihedral angle potential describes the angular spring between the planes formed by the first three and last three atoms [33] Dihedral angles

are advantageous because internal coordinates naturally provide a correct separation of internal and overall motion. This was found to be essential for the construction and interpretation of the free energy landscape of a biomolecule undergoing large structural rearrangements [2]. It can be defined as two non-collinear vectors lying in the plane; taking their cross product and normalizing it yields the normal unit vector to the plane. Thus a dihedral angle can be defined by four, pairwise non-collinear vectors. The torsion-angle molecular dynamics method in principle allows for the inclusion of other functional forms. The figure below is a good illustration of the potential energy dihedral angles can exert:

2.2.3 Van der Waals

Van der Waals forces are the attractive or repulsive forces between molecular entities other than those due to bond formation or to the electrostatic interaction of ions or of ionic groups with one another or with neutral molecules. The term includes: dipole–dipole, dipole-induced dipole and instantaneous induced dipole-induced dipole forces.

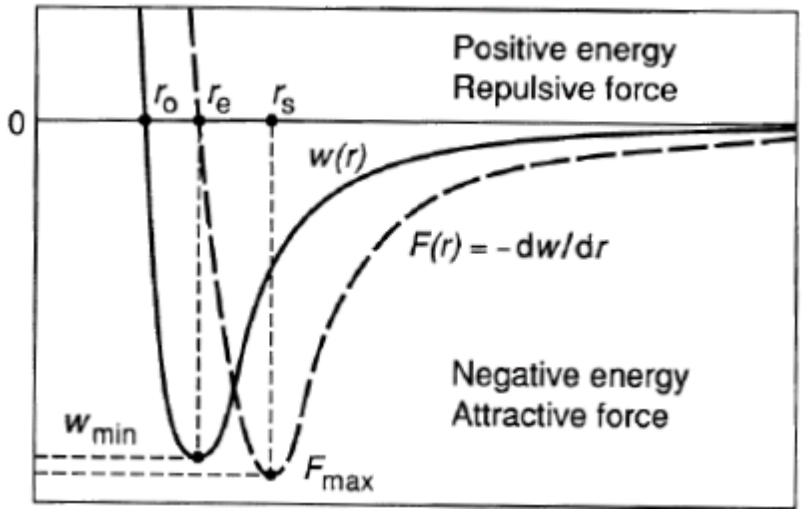

Figure 2.3: The graph demonstrates the principle of van der Waals forces. The attraction is the dominant component at a long range, while the repulsive force increases in intensity approaching atoms between them [1].

The electron motion around the nucleus allows one to consider the atom as an induced dipole – induced dipole force. As can be seen from Figure 2.4, attraction is the dominant component at a long range, while the repulsive force increases in intensity approaching atoms between them. From the graph above we can draw certain conclusions. One is that at r_s the potential energy is void and therefore the force

the dipoles exchange is zero. At this point the system can be considered balanced. At greater distances from the equilibrium, the potential energy goes to zero. The dipoles do not exchange energy and the repulsive force is attractive. At distances less than the equilibrium there is an increase in energy and the force is positive while the repulsive force is dominant [1].

2.2.4 Lennard-jones

The model most commonly used in molecular dynamic simulations is those of the Lennard-jones. The Lennard-Jones potential describes a very important concept in our study. It is a mathematically simple model that approximates the interaction between a pair of neutral atoms or molecules. It can be described by the following expression:

$$V_{LJ} = 4\varepsilon \left[\left(\frac{\sigma}{r} \right)^{12} - \left(\frac{\sigma}{r} \right)^{6} \right] = \varepsilon \left[\left(\frac{r_m}{r} \right)^{12} - 2 \left(\frac{r_m}{r} \right)^{6} \right],$$

where $\boldsymbol{\varepsilon}$ is the depth of the potential well, $\boldsymbol{\sigma}$ is the finite distance at which the inter-particle potential is zero, r is the distance between the particles, and r_m is the distance at which the potential reaches its minimum. This expression allows the system to have an equilibrated and stable system. The model of a single chain of chondroitin sulfate was developed to calculate and validate the Lennard-Jones parameters [10].

There are a few key principles that one relies on for the simulation to proceed correctly. One is that the simulation considers the electrons static. The force fields in NAMD do not take into account the state of excitation of the electrons. Instead it uses the approximation of the Born -Oppenheimer which makes each electron return to the idle state when changing the position of its reference atom. This limitation does not allow the simulation of all the processes that involves the transfer of electrons or their excitation. Another key point to consider is that the force field is approximated, and the most important factor to consider is that the simulation is based on the classical mechanics theory. Newton's laws of motion give an accurate description of the behavior of the atomic system in the range of physiological temperatures. There are limitations with classical mechanics that cannot be forgotten. Tunneling of protons can occur in hydrogen bonding, but the above method does not take this into account. The quantum oscillator significantly differs from the harmonic oscillator and at room temperature; all the bonds and bond angles are close to the limit, causing errors in the simulation. Therefore to remedy this a constant "correcting" term is inserted into the energy function that considers the bonds and bond angles constant during motion.

2.3 Structure and Modeling

The distinguishing factor about this study in comparison to others is that a full atomistic model is the subject of our experiment instead of a coarse grained model. Therefore all internal degrees of freedom including bond lengths, valence angles and torsional angles have the flexibility to respond as they naturally would in normal physiological conditions. The bulk solvation energy of the system was based on a previous experiment involving coarse grained chondroitin sulfate models. This physiological ionic strength proved to provide relevant results for that simulation and will now be applied as the initial ionic strength for this experiment. Figure 2.5 shows the molecular structure of CH, C4S, and C6S.

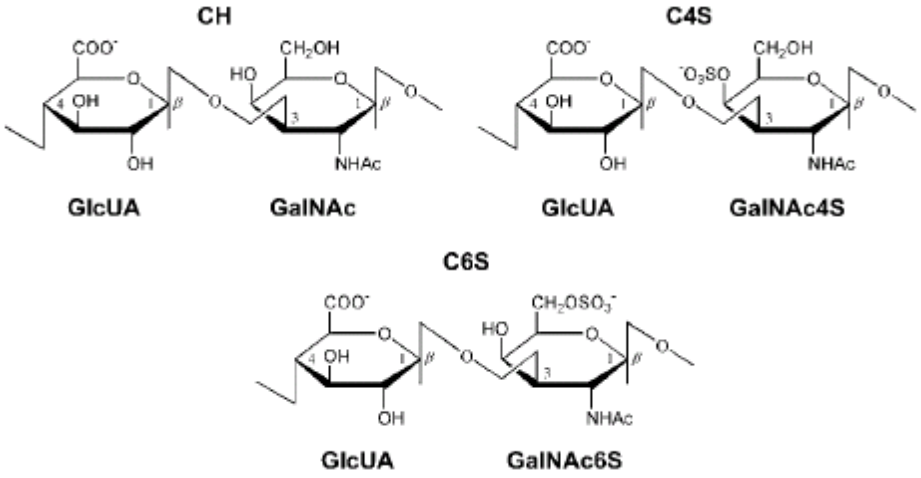

Figure 2.4: The above illustration shows the chemical structure of the disaccharides in question (CS, C4S, and C6S) [7].

2.4 Simulation Methods and Characterization

2.4.1 Summary

The influence of GAG's molecular parameters on their mechanical behavior was found using atomistic model simulations. Full-atomistic models are the most detailed models used in simulation. The molecules are represented as a number of atomic sites connected by chemical bonds. The interaction between these atoms is described by a potential, commonly known as a *force field*, which includes terms to describe bond stretches, bond angle bends, torsional rotations and non-bonded interactions. Simulations are performed via NAMD combined with the visualization platform VMD [41]. In order to

conduct meaningful computer simulations the environment with which molecules are presented must resemble that of the true environment. Therefore it is important to make the simulation as accurate as possible to the environment that one would encounter in real physiological conditions of chondroitin sulfate chains. In order to mimic this, the project was designed so that the chondroitin sulfate chains would have four and eight monomers. Each of which would have three different sulfation patterns. These would be composed of chondroitin-4-sulfate, chondroitin-6-sulfate, and chondroitin-0-sulfate. This makes six total chains that would be used as the platform for our evaluations and experiment. The first step in the process was to modify a script that was developed for a simulation of concentrated aqueous salt solutions in order to replicate an idea that would allow target molecules to be constrained within the boundaries enforced by the algorithm and let the untargeted variables escape [41]. In this case the targeted molecules were the chondroitin sulfate chains and the untargeted molecules were Sodium Ions. The script was modified in order to have infinite rectangular walls that would move inwards towards the chains to increase concentration of the environment and evaluate the characteristics the chains undergo.

The arrangement of the chains in the system had to imitate the natural physiological conditions. In order to do so, six systems were formulated each with four chains each. The chains of each individual system were identical in length and sulfation position. The chains in the system were placed at specific positions relative to each other. The chains were placed two nanometers apart from each other in each direction. This was done in order to get a precise read on the mechanical properties that are exerted on the chains as they are compressed. The chains were placed in a cubic water box with lengths of 74 x 74 x 74 Angstrom. The water box was infused with sodium ions in order to account for the negative charge of the chains.

The generation of each of the chondroitin sulfate chains was done using a previously developed Tcl script that was slightly modified in order to account for all sizes of the chains. This script was able to generate the desired atomistic models we wanted to build in VMD.

Visual Molecular Dynamics is a molecular visualization program for displaying, animating, and analyzing large biomolecular systems using 3-D graphics and built-in scripting [34]. It includes tools for working with volumetric data, sequence data, and arbitrary graphics objects. The valuable use of this program for the project at hand was that it allowed the manipulation and analysis of the GAG chains and their environment. In this experiment, VMD was used to visualize the chain and setting up the system. It was necessary in order to turn the Tcl script into an actual visual simulation.

NAMD (**N**ot (just) **A**nother **M**olecular **D**ynamics program) is a molecular dynamics simulation package written using the Charm++ parallel programming model. It is noted for its parallel efficiency and often used to simulate large systems of atoms. In this experiment NAMD was used extensively in order to simulate the ideal environment that will influence the GAGs mechanical behavior.

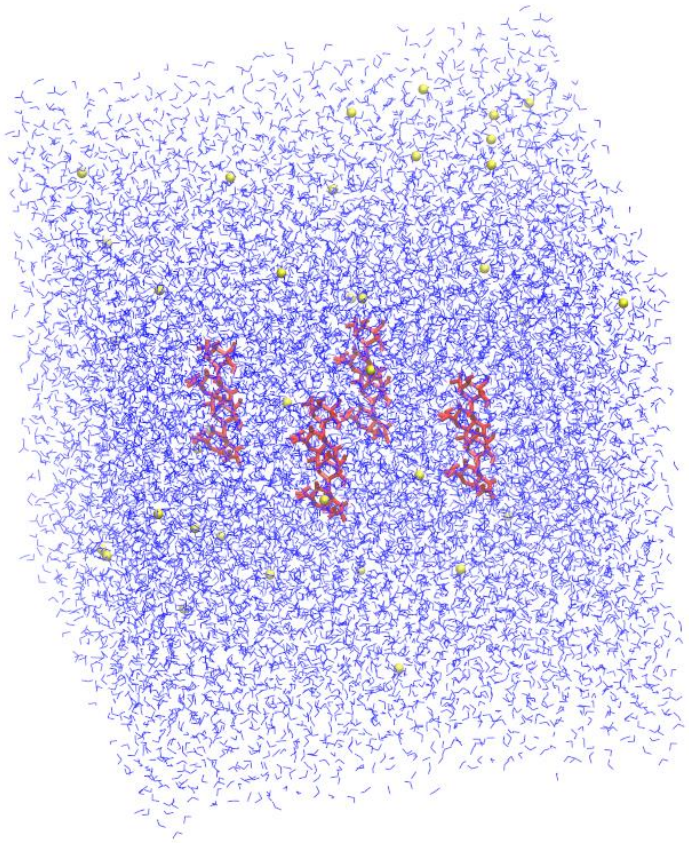

Figure 2.5: The illustration above is a representation of the system was generated. The Chondroitin Sulfate chains are represented in red for this illustration for visual purposes. The water molecules that surround the CS chains are TIP3P water molecules generated by NAMD. The sodium ions in the system are represented in yellow.

2.4.2 Specifics about configuration file

The configuration file contains all the specifics about the simulation that will be run. The configuration file is parsed by NAMD using the Tcl scripting language that is case sensitive and order-independent. The whole file is parsed until NAMD reads the minimize command. From this point the input files are read and the calculations begin.

The first commands of this config file give the coordinates and structures through PDB and PSF files. The temperature was initially set to room temperature in order to imitate physiological conditions, and was held constant throughout the simulation process to mimic GAG environment positions. The *outputname* command is crucial in the file because it provides the necessary information for NAMD to create a trajectory file (.dcd .xst), output file (.coor, .vel, .xsc), and a restart point. The parameter files are mostly specified by the CHARMM force field, but there are certain characteristics that must be specified for chondroitin sulfate specifically. These are called upon by NAMD and are also specified within the config file itself. The *cutoff* command is one of these parameters that must be specified. Since the Particle Mesh Ewald Sum is invoked in this config file the cutoff command has a different definition then if it PME was off. It dictates the separation between long and short range forces for the method. It does not simply cut off the forces but instead modulates them in order to get more accurate results. Particle Mesh Ewald Sum (PME) is a useful method for dealing with electrostatic interactions in the system when periodic boundary conditions are present [53].

Since our simulations are periodic and require long range force calculations, PME provides an efficient manner for calculating force. It is essentially a 3D grid created in the system over which change is distributed. Potentials and forces on atoms are determined from this charge. The PME values were chosen in order to not slow down the simulation but have a large enough grid spacing to accurately represent charge distribution. Another force-field parameter implemented includes the *exclude* command, which specifies which atomic interactions are to be excluded from consideration [53]. This is important for our simulation in order to rule out the unneeded information and only focus on the necessary information. For our simulation we are interested in knowing the relationship that the GAG's experience in relation to the pressure being applied. This is the central goal of the simulation, therefore interactions between neighboring atoms is not as essential as getting the interactions of the whole GAG. This method allows for computational time and cost efficiency. Other parameters, including *switchdist, pairlistdist,* and *timestep* were placed into our config file in order to get accurate van der Waal and electrostatic interaction results, while maintaining efficient computational time constraints.

Molecular Dynamic simulations solve Newton's laws in a discrete approximation to determine the trajectories of atoms. The *timestep* function tells NAMD how to discretize the particle dynamics. In our case we used the standard 2 femtoseconds as an initial number and manipulated it as the simulation advanced to get optimal results. A timestep of any simulation should be dictated by the fastest process taking place in a system, which in this case is the movement of the atoms. Among these, the fastest interactions include bond stretching and angle bending, with typical bond stretching vibrations in GAG's occurring at 10 femtoseconds. Setting the *timestep* to 2 fs demands that these bonds be fixed

and the simulation takes into account only slower moving vibrations. Since the GAG's are rather large molecules, bond fixing is acceptable as only the slower vibrations are providing the necessary information. The other integrating parameters implemented in this script insure that the computational time is reduced while keeping the data accurate and relevant. Another important characteristic that was used to get more accurate results is Langevin Dynamics. Langevin Dynamics is a way of controlling the pressure and temperature of a system by controlling the kinetic energy of the system. The expression for Langevin Dynamics can be seen below:

$$m_i \frac{d^2 x_i(t)}{dt^2} = \mathbf{F}_i\{x_i(t)\} - \gamma_i \frac{dx_i(t)}{dt} m_i + \mathbf{R}_i(t)$$

This expression when applied to the GAG chains says that the ordinary force applied to the GAG's is equal to the sum of the frictional damping that is applied to the system with a frictional coefficient plus the random forces that act on the GAG as a result of solvent interaction [10]. Langevin dynamics is an important factor in our simulation in order to keep the temperature at a constant value. An important detail about this code is the outputs it renders. Although it may seem trivial without setting the right parameters for these files we run the risk of running a simulation and having no useful data. Therefore a restart frequency was made every 1000 steps in order to save the coordinates that the simulation was running and be able to restart from that point after a pause. The dcd file contains very important information regarding the trajectory of our system.

The *outputenergies* and *outputtiming* commands specified when to print the energies and the printing of performance. The script was set to every 1000 step in order to save time and every 5000 step to print time performance.

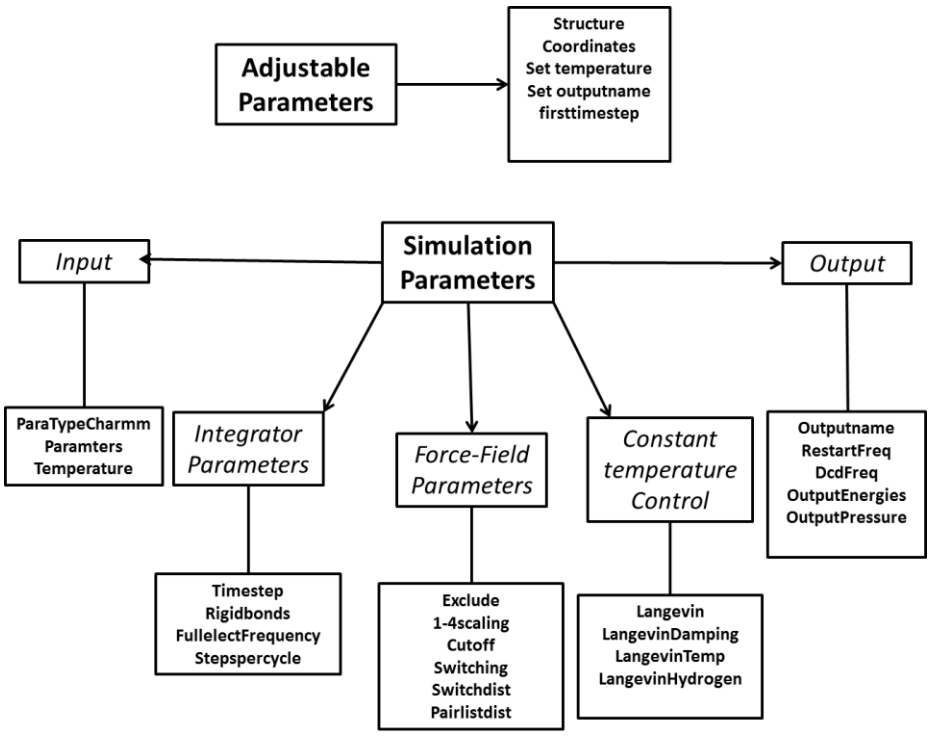

Figure 2.6: The scheme above shows the parameters in the Tcl script divided into different categories. The function of these parameters is explained in section 2.4.2.

2.4.3 Validation Techniques of Configuration File

In order to validate that the chain systems are in the correct environment and are being simulated correctly, a pre-experiment was simulated in order to make sure that our working scripts are functioning as they should. The environment that was setup is composed of NaCl ions placed in a water cubic box environment with the physiological temperature that the CS chains would undergo. A water box was built using the solvation box function in VMD with a volume of 110592 Angstrom^3 and cubic sides of 48 Angstrom. Then this box was solvated with Sodium and Chloride ions in order to have the desired concentration. The concentrations that were aimed for in our systems were set to .5, 1, 2, 3, 4, and 5 M. The system was followed by a minimization and a 2000 ps equilibrium simulation at constant temperature with Langevin dynamics and periodic boundary conditions.

The same setup as the CS chains was established and a semipermeable membrane was applied to the system to keep the ions within the constraints and a force constant of 10 kcal/mol/A^2 was used. The water molecules had no restraint applied to them and could move freely throughout the periodic system. The virtual vertical walls constrained the ions in the z direction and was setup using the Tcl

script in NAMD that will be discussed in section 2.5. Then the results from each simulation were analyzed and a force vs concentration plot was created. The created plot displayed very similar results to that of Luo and confirmed that our virtual membrane script was running correctly.

2.4.4 Construction of GAG systems

The constructions of the CS chains are summarized below. Just like any other molecular dynamic creation there are rules that must be kept and enforced. The force fields of the molecules and their mapping must be kept in order and is based on the C6S parameters specified in Clipa eg at [17]. The basic parameters for the disaccharides were determined and it was checked for errors in a displayed environment (VMD). In order to make distinctions between atoms easier and further create connecting disaccharides, specific groups were highlighted. Further the chains used a force field for aggrecan as a base in order to parameterize the chains. The parameters were extracted and the molecule defined. After these steps were completed the chains could be created to be any length depending on how many disaccharides the user wants.

Now that the chains can be created at will, it is important to validate the model. Therefore the chain was created and tested in a solvent and in a vacuum. When testing in a solvent it is important to define an appropriate box which contains the chain and then insert the solvation box over it. It is important to account for the “low” and “high” values because each can produce different problems. Ultimately, the molecule distances were set equal to the cut off value for Van der Waals. In this case it was set to 1.2 nm. Once the system was ready for testing the chain, the minimization steps for the chain were initiated. The chain was then balanced just like any other system in order to ensure that is fits to literature results and to get the ideal temperature and pressure. The reason for these operations involves the simulation of real physiological conditions. The temperature in this experiment is in charge of a change in kinetic energy of the system. The system must also have a proper density in order to proceed with the system.

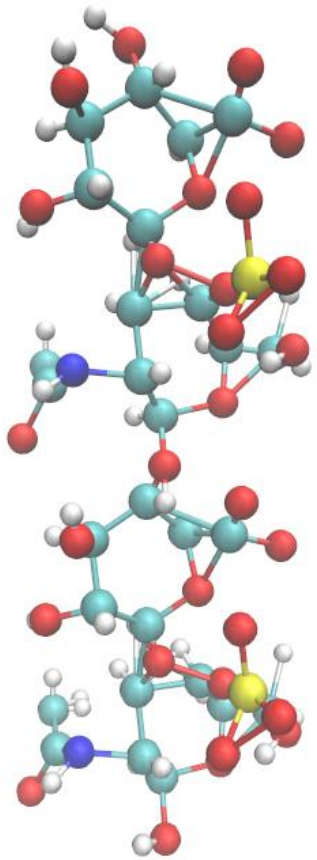

Figure 2.7: A chondroitin-4-Sulfate chain visualized in VMD software. The teal color represents the carbon atoms, red represents the oxygen atoms, yellow represents sulfur atoms, blue represents nitrogen atoms, and white represents hydrogen atoms.

In standard physiological conditions, CS undergoes a compression during the act of flexion. The GAG chains are compressed and this causes a variety of compressive forces to act upon the chains. In order to gain insight into these forces, specifically osmotic pressure, simulations of the GAG chains in physiological conditions were setup. It was not enough to just compress the chains, but an environment simulating the reality of GAG chain interactions was created. In order to do this solvation and ionization would have to be simulated for different concentrations and chain sizes. The chains were manipulated in order to have the membranes enclose on the GAG chains in the z direction. The chains were setup 2 nm apart from each other because this is the most accurate spacing of the chains observed. Each atom in the chain had a distance of 2 nm from the clone atom on the other chain therefore they were not in a perfect square but were oriented in a tetrahedral. In order to do this, two chains were

loaded into VMD and one was shifted 20 Angstrom in the x direction. This created two parallel chains in the x direction. These two files were merged creating one PDB and PSF file.

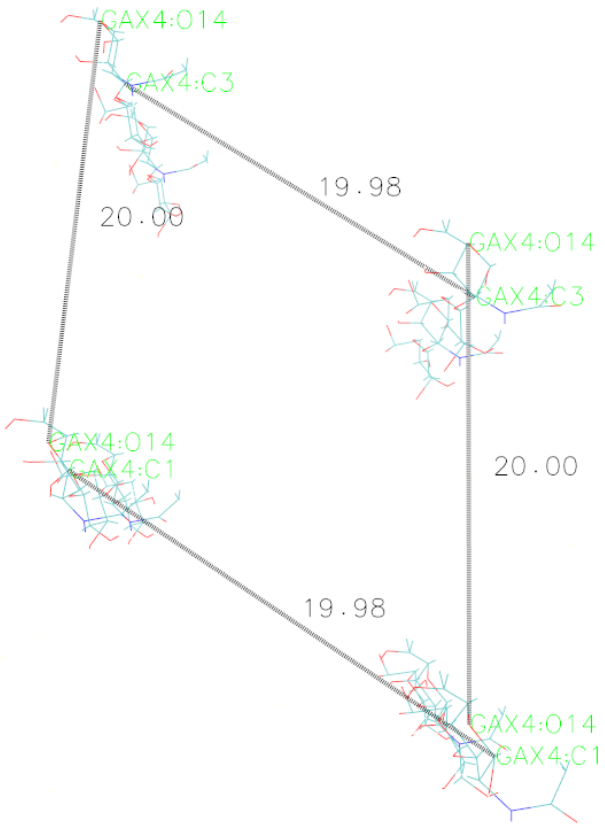

Figure 2.8: The figure above shows the distance from atom to atom on each CS chain. The system was composed so that each chain (and thus each parallel atom on each chain) is 2nm from each other, in order to imitate the physiological environment in articular cartilage.

Then the new PDB file was loaded into VMD twice and the top PDB file was moved 10 nm in the x-direction and 17.3 nm in the y-direction according to the Pythagorean Theorem. These distances were specified in order to provide each chain with a 2nm distance from molecule to molecule. The two chains with the new coordinates were merged with the first two chains at the initial position. This provided a system of GAG chains with an all-around distance of 2nm from chain to chain.

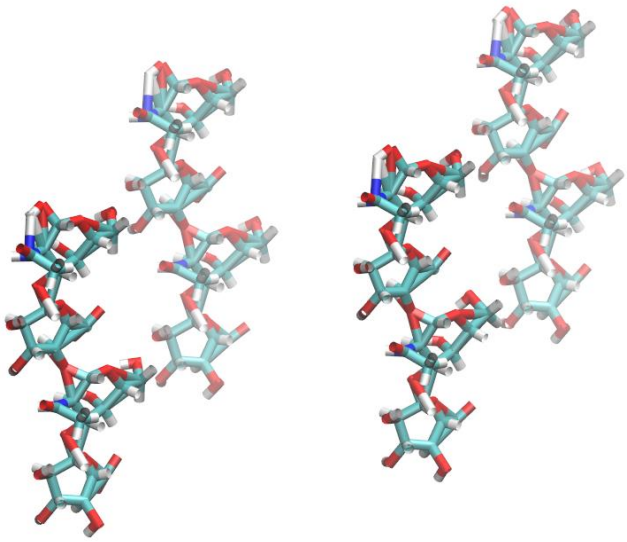

Figure 2.9: The illustration above gives an accurate display of the organization of the four Chondroitin Sulfate chains at 2nm apart and parallel to the z-axis.

Running a compression simulation on just these chains would provide a good amount of information, but the overall goal of this project is to get the osmotic pressure therefore further manipulations had to be made. In order to get this force we must simulate a physiological condition similar to that experienced in the extracellular matrix of the cartilage. VMD provides a periodic environment for a solvation box, therefore the lengths of a solvation cube were calculated for each system based on the volume, mass, and desired concentration. The mass of a disaccharide was specified as 457 Dalton/disaccharide according to previous studies. Given this information and the equation below, one can find the volume of the box.

$$\rho_i = \frac{m_i}{V}.$$

Where m_i is mass, V is volume, and p_i is molar concentration [26]. The concentration of sodium ions in each system is very important to the simulation because the concentration must replicate that of the extracellular matrix. In order to find the amount of sodium ions needed for each concentration, Avogadro's number was used. The initial physiological concentration at rest is .15 M and is simulated in the experiment. The volume for the solvation box used on the four monomer chain system had

different dimensions than the volume of the eight monomer chain system. This was within our predictions and can be verified by the equation above. In order to simulate a physiological environment, not only do the GAG chains have to be surrounded by water but ions must be added in order to imitate extracellular matrix conditions. Therefore environment concentration was controlled by sodium ions and the semipermeable membranes that impose force on the GAG chains. The concentration of .15 M was used for the initial simulation and movement inward on the x axis by the semipermeable membranes provided an increase in concentration.

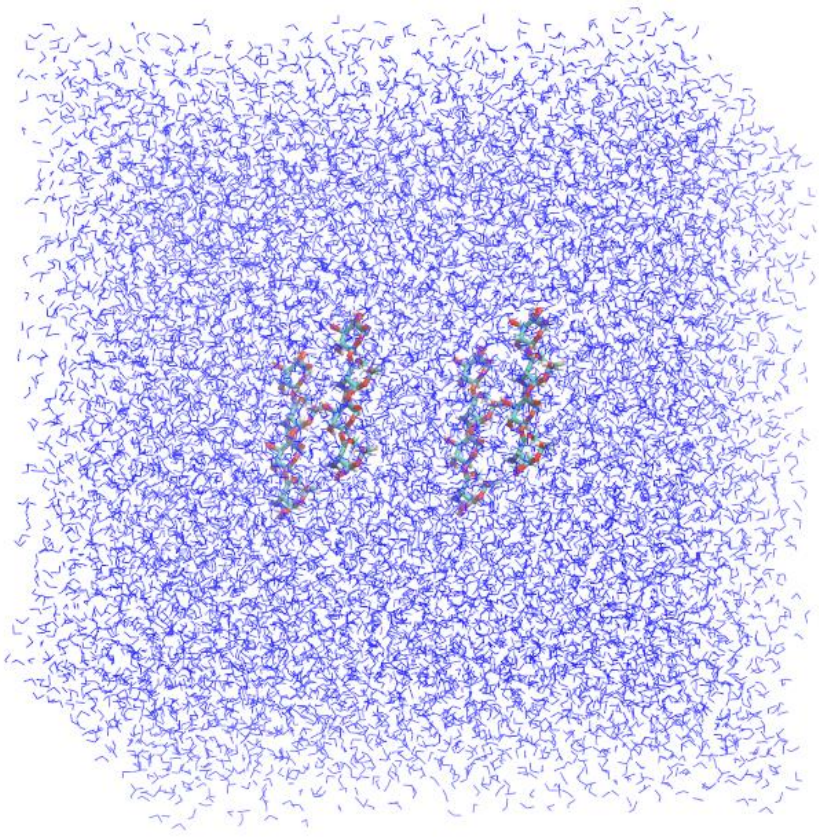

Figure 2.10: The system above is the final system design. The illustration shows the orthogonal box with four CS chains inside. The semipermeable membrane is initially at the edge of the box but as concentration changes so does the membrane.

The simulations were run on multiple processors for faster processing of the long simulation times. Each processor calculates its own force, therefore in order to get the total force the sub processor forces

must be added together. A simple script was created in order to add up the forces using the .log file created at output. The script was a simple tool used to save time and find the total force created by each simulation.

2.4.5 Semipermeable Membrane Setup

The semipermeable membrane was written so that the atom that represented water and sodium would not be affected by the semipermeable membranes, while the GAG chains would be constrained. This script was written by modifying a previous script provided by the NAMD water sphere tutorial [54]. In that tutorial the x, y, and z direction all acted upon the sodium and potassium ions in a manner that would simulate a spherical inward trajectory. In this experiment, only one axis is used to constrain the GAG chains consequently the script was modified to take this into account. NAMD assigns a specific ID for each atom in its system. The water and sodium atoms were excluded from the force that would act upon the rest of the system (semipermeable membrane). It is a simple but useful method to impose a force on the desired compound without affecting the other atoms. Another important aspect that was taken into account in our simulation design was wall separation. The initial wall to wall distance determined the concentration that the simulation at hand would represent. This is an important concept because although we start the simulation at .15 M and go up to .80 M, the initiation of the walls at the concentration provides us with a more accurate picture of what is taking place within the extracellular matrix. This will be further discussed in upcoming sections. In order to account for this, the config file was altered so that it had a min and max position, instead of a radius as in the sphere tutorial.

The config file used to run the simulation calls a Tcl script that is responsible for the constraining of the GAG chains, essentially providing the data needed to calculate the osmotic pressure. The line set *avgNumIons* calculates the average number of ions found outside the sphere at each step. The command *wrapmode cell* takes the atom's equivalent position to its position in the input files of the simulation. Now we use the *proc calcforces* command which tells the *command tclBCArgs {}* located in the NAMD config file to not pass any arguments to calcforces. Then we define our variables with the command *global* including radius, force constant, avgNumIons, max, min, and deltaX. Now we start to make the logical argument for our semipermeable constraints. The PDB file for our ionized system of NaCl gave us specific atom id numbers representing the ions and water molecules. It is important to remember that NAMD is a very efficient program that places the atoms in order hence a small statement was made to constrain the sodium ions while letting the water atoms pass. The

command *if { [getid] < 10171 }* selects the atoms below the ID number. The statements set *rvec [getcoord]* and *foreach {x,y,z}* finds the ID's specified in the previous command and if they are present returns the position if not it is negligible. The next line *{set absX [expr (abs($x))]* is very important to the overall simulation because it finds the distance between the ion and the center of the membranes. The next few commands apply the force specified earlier to each ion in the z direction if it's outside the membranes. The components of the force vector are chosen so that the vector is directed towards the membrane center taking into consideration, the negative and positive side of the membrane. The last few commands account for the output of the system and the steps that need to be taken. In conclusion, the script is an essential part of the simulation because it states that all of the atoms less than the specified atom ID (GAG chains) will be constrained and those above the specified ID (water molecules) will be free to move. The constraint is moved only in the z direction while leaving the x and y constraints permanent and without motion at the boundaries of the solvent box [53].

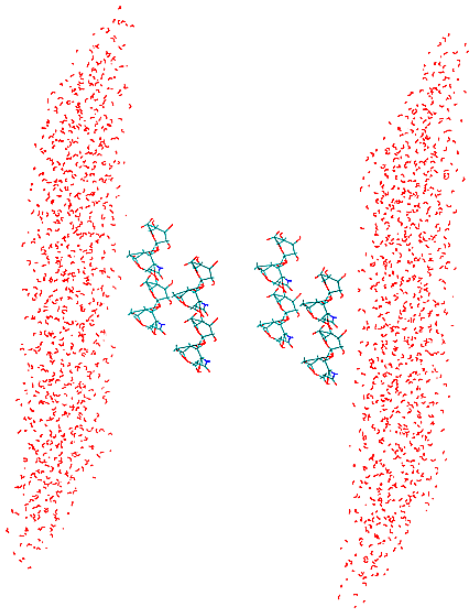

Figure 2.11: The red molecules to the right and left of the GAG chains represent the invisible semipermeable membrane that will induce a force on the chains. The semipermeable membranes and the GAG chains are parallel with the z-axis; therefore a perpendicular force is placed on the GAG chains. The water molecules have been removed to show a clearer picture of the semipermeable membranes.

2.4.6 Osmotic Pressure

The osmotic pressure is the pressure that has to be applied to a pure solvent to prevent it from passing into a given solution by osmosis. Osmosis is the spontaneous movement of a solvent from an area of low solute concentration to a region of high solute concentration [51]. The osmotic pressure depends on the molar concentration of the solute but not on its identity, meaning that it is a colligative property. The driving force behind osmosis has been commonly misunderstood but it is now understood that osmosis requires a force in order to function [19]. The force is supplied by the solute's interaction with the surrounding membrane. Brownian motion accounts for the random motion of solute particles in a solution so in order for there to be a process such as osmosis, it is only logical that a force is exerted [6]. The explanation for osmosis can be seen from Figure 2.11 below.

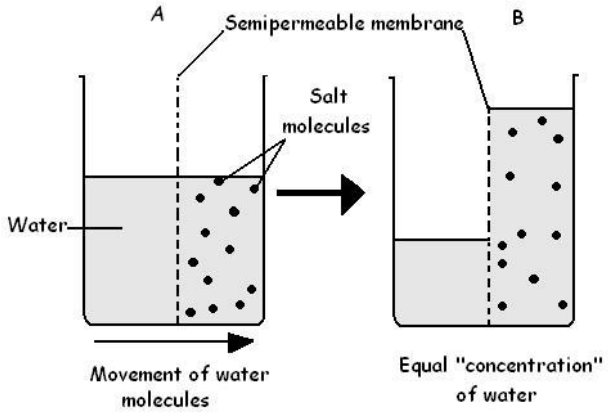

Figure 2.12: The illustration shows the effects of osmosis. The water moves from an area of low solute to an area of high solute in order to have an equal "concentration" on both sides of the semipermeable membrane [52].

As the solute particles move toward the pores of the semipermeable membrane they are repelled and acquire a negative momentum away from the membrane. This leads to the practice of the first law of thermodynamics which states that the total energy of an isolated system cannot change. The momentum applied to the solute particles is transferred to the surrounding environment (water molecules), driving the water molecules away from the membrane [38, 52].

It is important to understand this concept, in order to comprehend why the osmotic pressure is such an important characteristic of the GAG chains. Osmotic pressure is important physiologically because it

determines the distribution of the water in the body between different fluid compartments. The extracellular matrix compartment is divided into two compartments known as the intravascular and interstitial compartments. Both compartments have important functions that are filled with different fluids [19]. The intravascular compartment is filled with circulating plasma water while the interstitial compartment is filled with interstitial fluid which consists of a water solvent containing sugars, salts, fatty acids, amino acids, coenzymes, hormones, neurotransmitters, as well as waste products from the cells. Since all cell membranes and peripheral capillaries are permeable to water, the distribution of water between these compartments is entirely determined by osmotic pressure [6].

Therefore to know what happens within cartilage when a Chondroitin sulfate chain is compressed, it is important to know the osmotic pressure. To find the osmotic pressure of the GAG chains the following equation was used.

$$P = \frac{F}{A},$$

where F is force and A is area. First, the average force imposed by the axial force when the GAG chains were compressed and achieved stability within its limits, was calculated at each concentration. This step was conducted in order to validate our results and check for errors. The force that NAMD outputs is in kcal/mol-angstrom, but pressure is in Pascal therefore the force was converted to Newton's and the area was converted to meters squared. Once these conversion factors had been carried out, the pressure was calculated and plotted on a pressure vs molar concentration graph. This pressure is determined to be the osmotic pressure because of the behavior that is taking place within the simulation.

Chapter 3

RESULTS

3.1 Initial Validation Techniques

The initial validation techniques used for confirming the parameters specified in our system proved favorable. The data was compared to that of Luo and Roux e.g. al [41] and similar results were surveyed. Figure 3.1 shows the calculated osmotic pressure for the NaCl ion solution and compares both the data acquired from this study and the data from Luo, plotted on a pressure (bar) vs concentration (M) graph. From the results we can see that the MD simulations matched those attained up to 3M [41]. Above 3M there were significant drops in congruity due to an excess of ion pairing at the high concentrations.

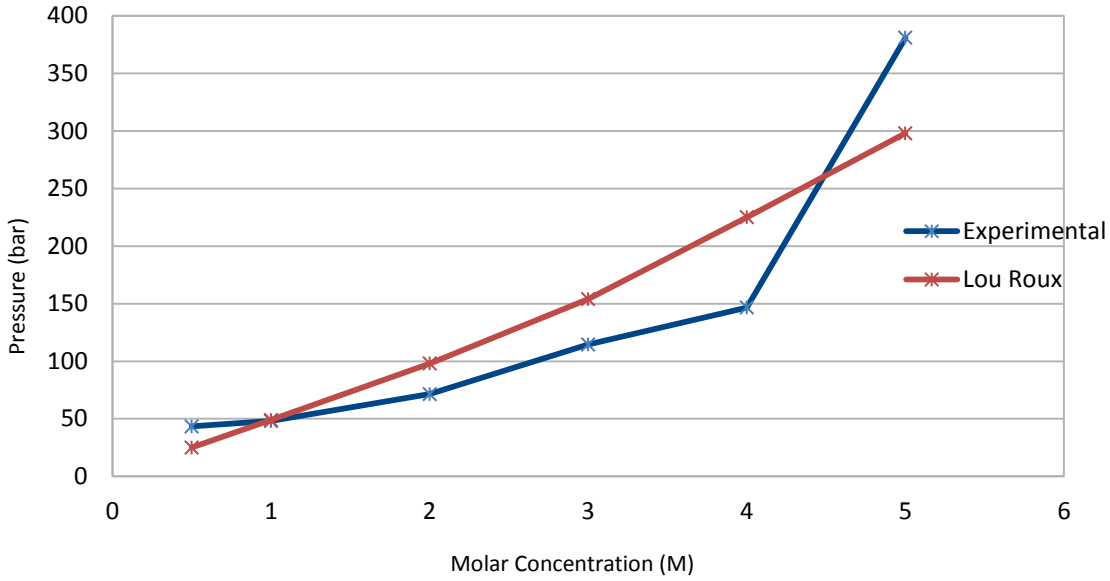

Figure 3.1: Comparison relationship between the osmotic pressure attained from experimental techniques vs. the data acquired by Luo and Roux, plotted as a function of molar concentration for the NaCl ions in TIP3P water molecules.

As we can see the data follows the general trend observed in the Roux et al. experiment but had slight discrepancies [41]. The discrepancies are attributed to the fact that they used an NBFIX on Na+ by recalculating the R^{ij}_{min}. The main purpose of this study is to calculate the osmotic pressure of CS chains therefore the relationship between both data sets was evaluated up to 3M, beyond this point would be computationally expensive and inadvisably time consuming. The small discrepancies between .5M and 3M are attributed to differences in parameters and force fields. The tools used to conduct Luo and Roux experiments were different than that used in this study including the parameters which are revised from CHARM PARAM 27 to CHARM PARAM 36 [41].

3.2 GAG Chains

The membrane was observed to act as hypothesized and kept stable during the simulation with no extensive deviations, performing its purpose with excellent results. From the trajectory file produced by the simulations, it was observed that the GAG chains exhibited axial force behavior in the x-direction and can be seen from the figure below.

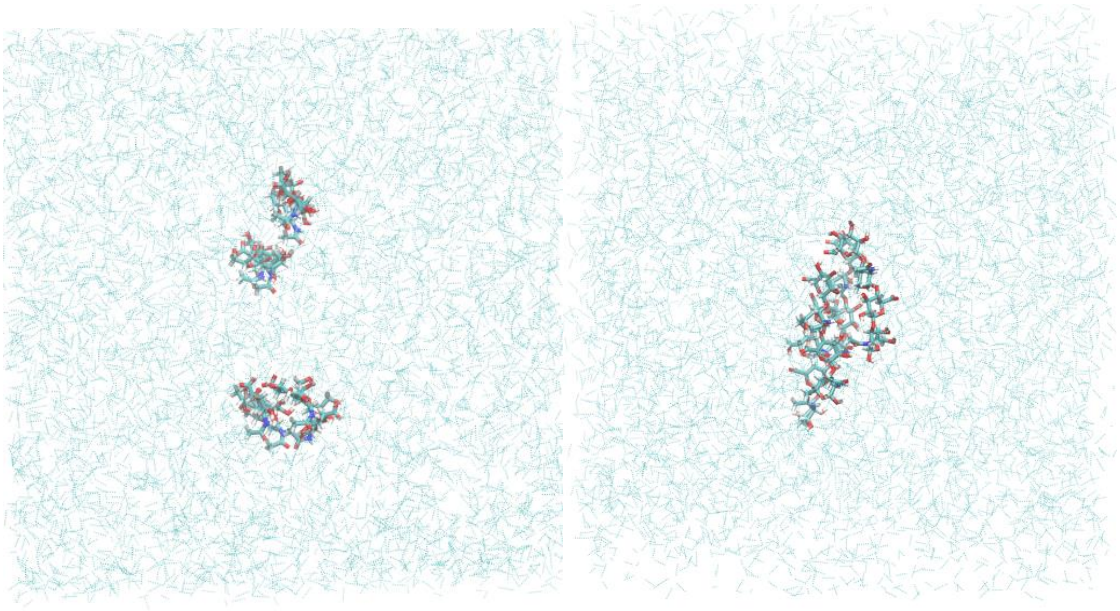

Figure 3.2: The compression of the chains by the semipermeable membrane can be seen from the two screenshots above. Illustration on the left shows the chains compressed in the top view of the solvent box. Illustration on the right shows the chains being compressed from the side view.

In order to verify that constrained artifacts were not a cause for discrepancies, a larger system with dimensions of 96 x 96 x 96 Angstrom^3 was created and a system consisting of Chondroitin-4-Sulfate chains was inserted as before. The simulation was run for the same concentrations and the results were in excellent correlation with the results of the smaller system.

The LJ parameters specified by CHARMM PARAM 36 force field's used in this study were not modified as in previous studies because the membranes are composed of net neutral molecules. Therefore the parameters specified by the parameter field are excellent fits because the differences are negligible for our CS chains and suit our purpose of finding the osmotic pressure.

The convergence of the system was determined after letting the GAG chains rest within the membrane space for a reasonable time. This required more computational cost but provided more accurate results because the CS chains are now experiencing the complete force within the solvent instead of a partial pressure, allowing its properties to experience the full force of the desired concentration. Once the proper range of data was established, interpretation of the data was executed via RMS and Mean Average.

The first simulation was conducted with C4S using a 1 kcal/mol-Angstrom force constant. The data in Figure 3.3 shows that the data attained was sparse and infrequent. This was due to the high force constant, Therefore a smaller constant was used in order to gain more data from contact forces, to remediate this problem. The force constant was decreased to 0.1 kcal/mol-Angstrom and results showed a 1.34% error between 1 and 0.1 kcal/mol-Angstrom. This process was repeated for .30M and .45M with each providing percentage error of less than 1.20%. Table 3.1 shows the acquired average mean and RMS for both .01 kcal/mol-angstrom force constant and 1 kcal/mol-angstrom force constant. As we can see the forces are quite similar and the regression line proved very useful in continuing with data analysis.

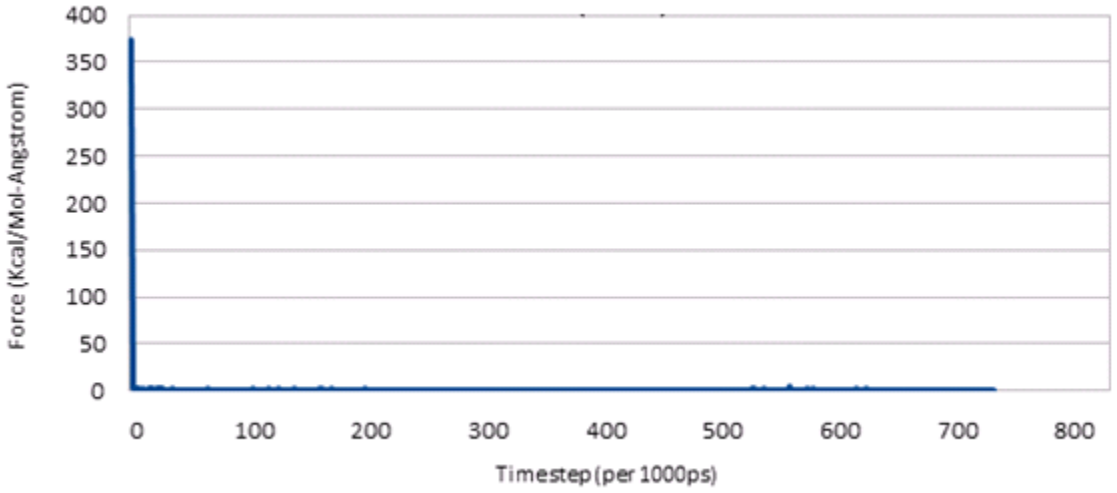

Figure 3.3: This plot shows the relationship between force and timesteps for a four monomer C4S system at 0.15 M concentration for a 1 kcal/mol-Angstrom force constant.

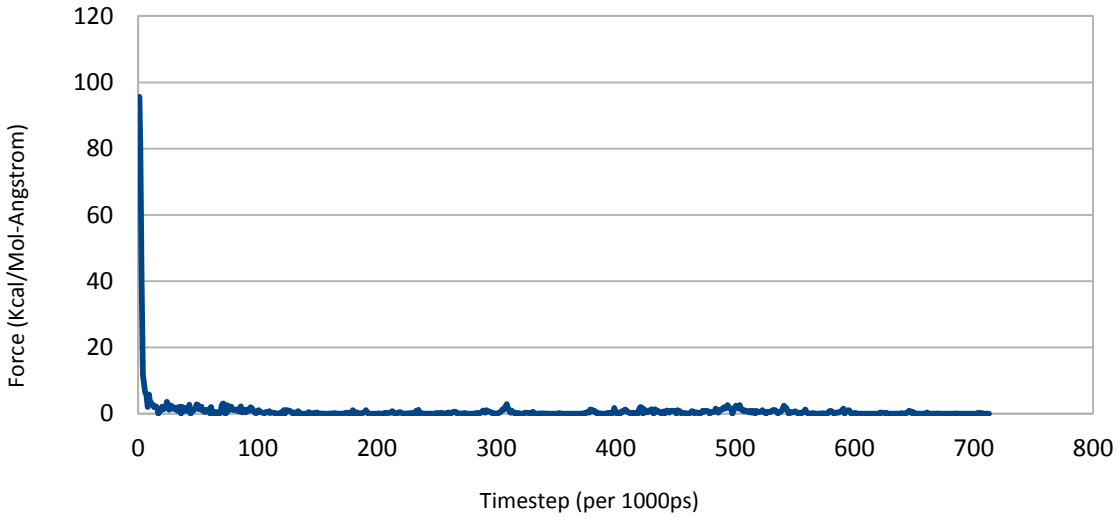

Figure 3.4: This plot shows the relationship between force and timesteps for a four monomer C4S system at 0.15 M concentration for a 0.1 kcal/mol-Angstrom force constant.

Molar Concentration (M)	Average Force for 1 kcal/mol-Angstrom	Average Force for 0.1 kcal/mol-Angstrom
0.15	0.18531484	0.16224684
0.3	0.32606224	0.294547782
0.45	0.512998063	0.488508286

Table 3.1: The table above shows Average Force attained for the C4S 4 monomer system from two different force constants.

After repeating this process with .30 M and .45 M and finding excellent data matching (refer to Table 3.1) the rest of the simulations were conducted with a force constant of 1 kcal/mol-Angstrom. The average force was plotted as a function of concentration and was found to be as expected. Figure 3.5 shows a faint linear relationship from .15 M to .45 M with an increase in the slope from .45 to .80 M for C4S.

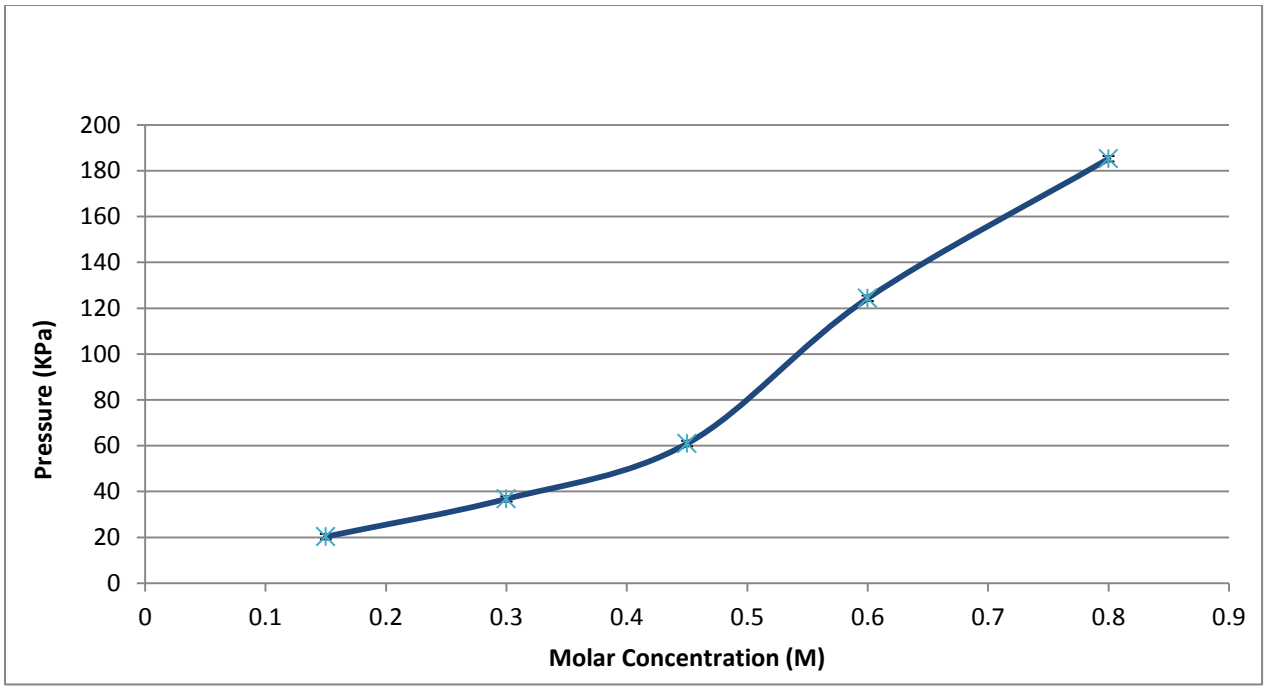

Figure 3.5: Pressure vs. Molar Concentration for the C4S 4 monomer system. Statistical error bars are smaller than the symbols.

Molar Concentration (M)	Average Force (Kcal/Mol-Angstrom)	Area (Angstrom^2)	(kcal/mol-Angstrom^3)	Pressure (Pa)	Pressure (KPa)	Standard Deviation	Coefficient of Variation
0.15	0.16	5476	2.92184E-05	203004.29	20.32	0.21	1.32
0.3	0.29	5476	5.29584E-05	367945.28	36.79	0.37	1.28
0.45	0.48	5476	8.76552E-05	609012.87	60.9	0.73	1.53
0.6	0.98	5476	0.000178963	1243401.3	124.34	1.38	1.41
0.8	1.46	5476	0.000266618	1852414.2	185.24	1.51	1.03

Table 3.2: Table for Chondroitin-4-Sulfate for the 4 monomer system showing the necessary parameters needed to find the Osmotic Pressure and showing the Standard Deviation.

The next important task to be tackled is that of simulating chondroitin unsulfated and chondroitin-6-sulfate under the same concentrations. For consistent data acquisition, the same method used to setup the 4-sulfated chondroitin sulfate chain system was used for the CS and C6S systems and the same parameters for simulation were setup. The Pressure vs. Molar Concentration Graphs for C6S and CS can be seen in the Figures below.

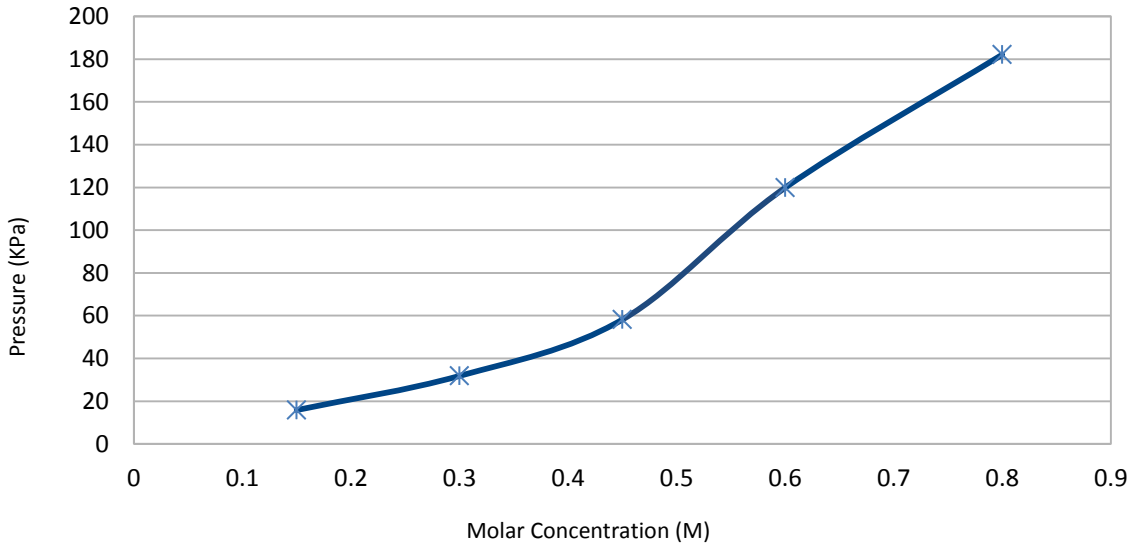

Figure 3.6: Pressure vs. Molar Concentration for the C6S 4 monomer system. Statistical error bars are smaller than the symbols.

Molar Concentration (M)	Average Force (Kcal/Mol-Angstrom)	Area (Angstrom²)	Force/Area*1000000	Pressure (Pa)	Pressure (KPa)	Standard Deviation	Coefficient of Variation (Normalizing)
0.15	0.12	5476	22809.53	15847.66	15.84	0.15	1.25
0.3	0.25	5476	45800.58	31821.43	31.82	0.27	1.1
0.45	0.45	5476	83699.9	58153.2	58.15	0.52	1.14
0.6	0.94	5476	172522.15	119865.32	119.86	1.2	1.27
0.8	1.43	5476	262113.11	182111.52	182.11	1.54	1.07

Table 3.3: Table for Chondroitin-6-Sulfate showing the necessary parameters needed to find the Osmotic Pressure and showing the Standard Deviation.

The results show similar values between the 4 sulfation and 6 sulfation chondroitin sulfate chains. The osmotic pressure at each molar concentration has excellent resemblance, and the values are within one standard deviation of each other. This implies that the sulfation group has little bearing on the osmotic pressure of GAG chains. This will be further discussed in the Discussion section.

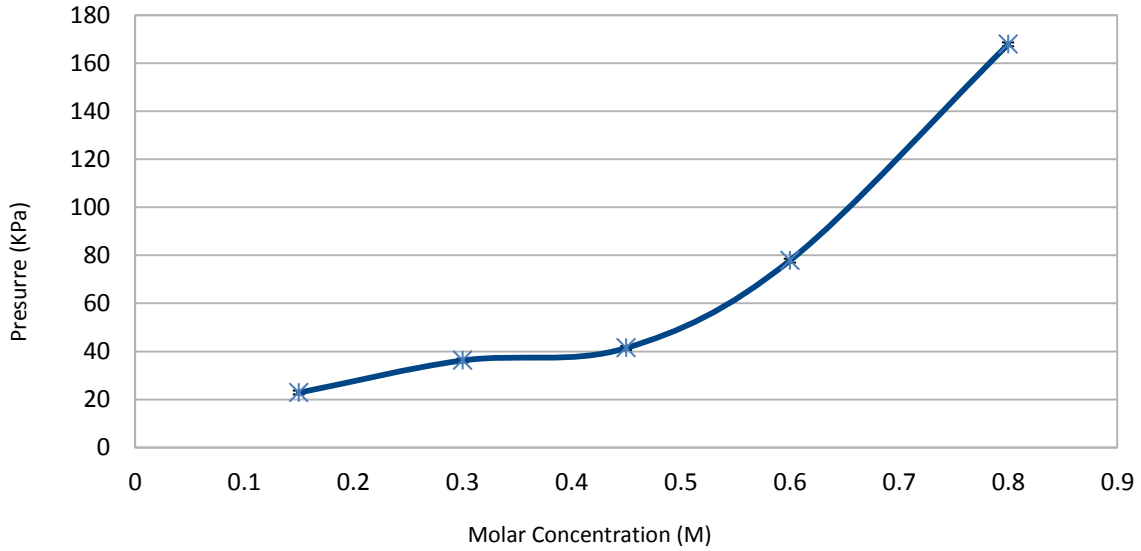

Figure 3.7: Pressure vs. Molar Concentration for the C0S 4 monomer system. Statistical error bars are smaller than the symbols.

Molar Concentration (M)	Average Force (Kcal/Mol-Angstrom)	Area (Angstrom²)	Force/Area*10 00000000	Pressure (Pa)	Pressure (KPa)	Standard Deviation	Coefficient of Variation (Normalizing)
0.15	0.2	5476	37206.78	258506.09	22.85	0.35	1.74
0.3	0.28	5476	52147.2	362309.46	36.23	0.43	1.53
0.45	0.32	5476	59634.39	414329.16	41.43	0.69	2.12
0.6	0.61	5476	112031.24	778373.11	77.83	0.86	1.4
0.8	1.32	5476	241554.38	1678276.85	167.82	1.5	1.14

Figure 3.4: Table for Chondroitin-0-Sulfate showing the necessary parameters needed to find the Osmotic Pressure and showing the Standard Deviation.

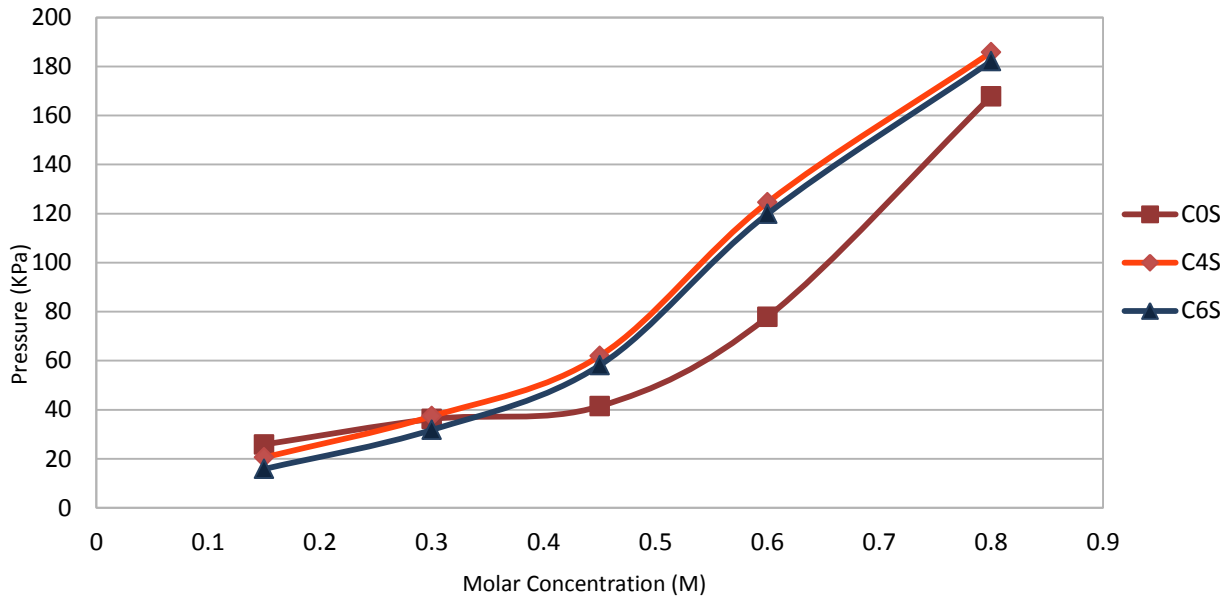

Figure 3.8: Comparison between three different CS sulfated chains (C0S, C4S, and C6S) for a 4 monomer system. C4S and C6S produce similar results while C0S has a slightly lower osmotic pressure than the other two chains at higher concentration.

3.3 GAG Chain Length Increase

Once this data had been thoroughly analyzed and squeezed for information, the next important question can be tackled. How can the information acquired be used to explain the characteristic of physiological CS behavior in a natural physiological environment? Chondroitin Sulfate chains are composed of between100 and 200 monomers. Consequently, for the data to be relatable to these lengths I hypothesis that by doubling the length of a CS chain one can find a relationship between length and osmotic pressure that can be used to analytically expand on the biomechanical behavior experienced within a physiological environment.

The length of the chains was doubled hence a four monomer system was increased to eight monomers with the same sulfation states as before. Once the three CS, C4S, and C6S 8 monomer chains had been built, the same procedure used to build the 4 monomer systems described above was carried out. The solvation box was increased to 93 Â by 93 Â by 93 Â and the number of ions in the system was doubled to 74 in order to replicate the environment experienced by the 4 monomer chains.

The figures below show the results for the three 8 monomer chains and they're pressure vs. molar concentration graph.

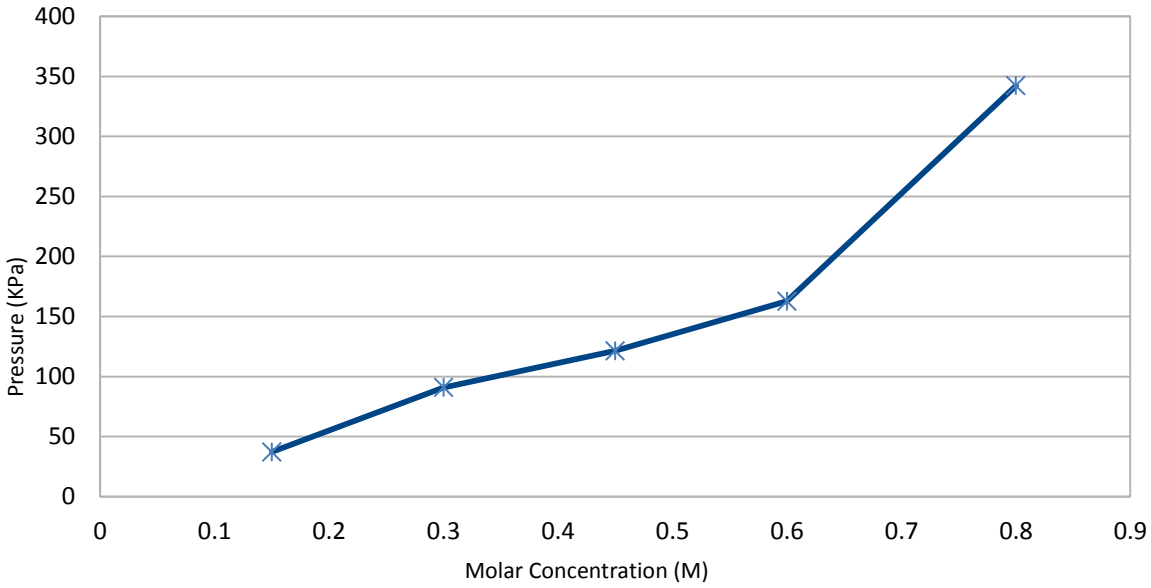

Figure 3.9: Pressure vs. Molar Concentration for the C4S 8 monomer system. Statistical error bars are smaller than the symbols.

Molar Concentration (M)	Average Force (Kcal/Mol-Angstrom)	Area (Angstrom^2)	Force/Area*10 00000000	Pressure (Pa)	Pressure (KPa)	Standard Deviation	Coefficient of Variation (Normalizing)
0.15	0.29	5476	53571.24	372203.44	37.22	0.59	2.01
0.3	0.71	5476	130872.88	909281.52	90.92	0.62	0.86
0.45	0.95	5476	174882.27	1215050.9	121.5	0.79	0.82
0.6	1.28	5476	234350.21	1628223.52	162.82	1.52	1.18
0.8	2.67	5476	492577.1	3422337.95	342.23	1.95	0.72

Table 3.5: Table for Chondroitin-4-Sulfate for the 8 monomer chain system showing the necessary parameters needed to find the Osmotic Pressure and showing the Standard Deviation.

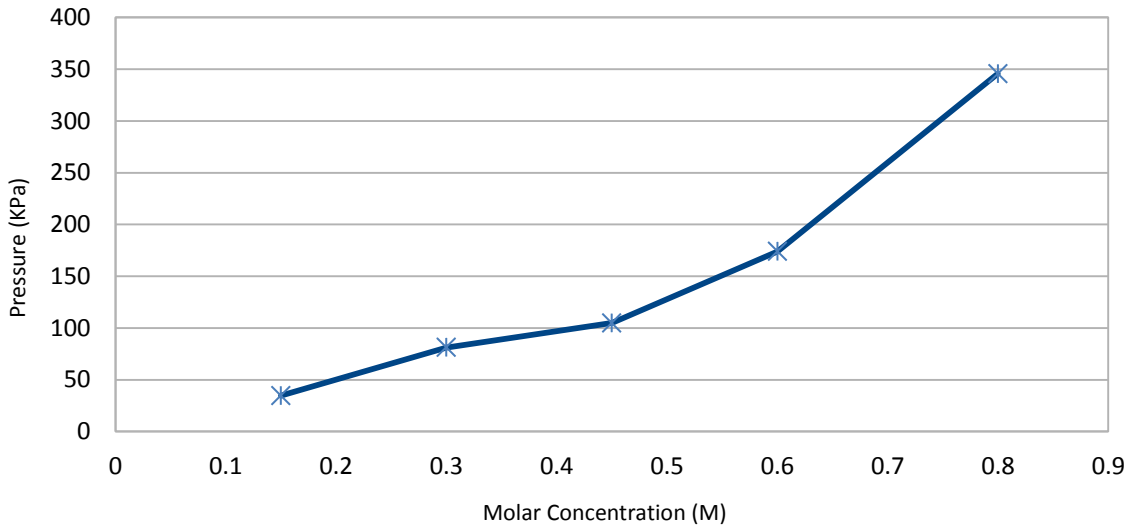

Figure 3.10: Pressure vs. Molar Concentration for the C6S 8 monomer system. Statistical error bars are smaller than the symbols.

Molar Concentration (M)	Average Force (Kcal/Mol-Angstrom)	Area (Angstrom²)	Force/Area*10 00000000	Pressure (Pa)	Pressure (KPa)	Standard Deviation	Coefficient of Variation (Normalizing)
0.15	0.27	5476	49944.78	347007.44	34.7	0.65	2.39
0.3	0.64	5476	117110.37	813661.98	81.36	0.69	1.09
0.45	0.82	5476	151011.58	1049201.62	104.92	0.77	0.93
0.6	1.37	5476	250240.13	1738623.85	173.86	0.92	0.67
0.8	2.72	5476	497551.68	3456900.43	345.69	1.75	0.64

Table 3.6: Table for Chondroitin-6-Sulfate for the 8 monomer chain system showing the necessary parameters needed to find the Osmotic Pressure and showing the Standard Deviation.

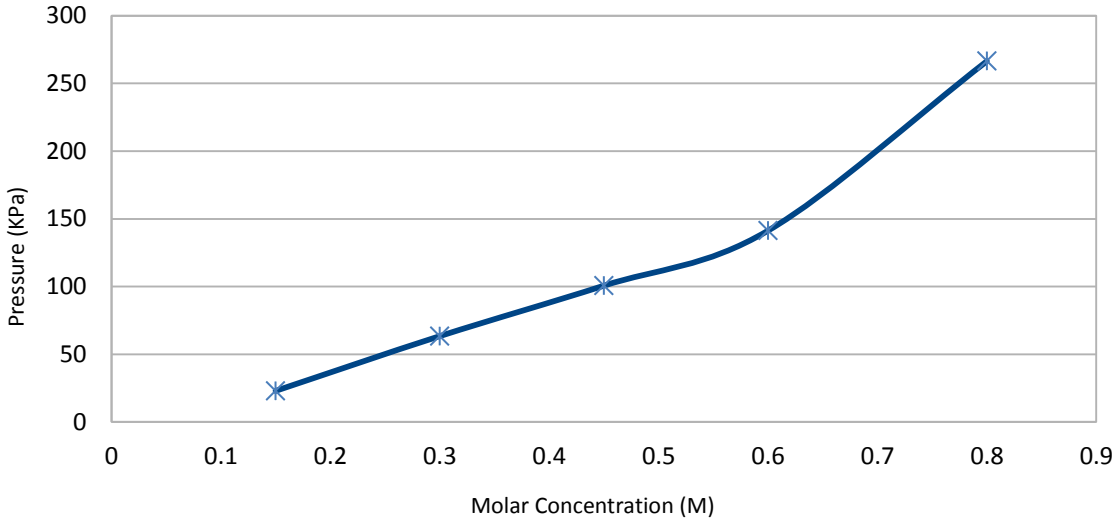

Figure 3.11: Pressure vs. Molar Concentration for the C0S 8 monomer system. Statistical error bars are smaller than the symbols.

Molar Concentration (M)	Average Force (Kcal/Mol-Angstrom)	Area (Angstrom²)	Force/Area*10 00000000	Pressure (Pa)	Pressure (KPa)	Standard Deviation	Coefficient of Variation (Normalizing)
0.15	0.18	5476	32976.09	229112.03	22.91	0.23	1.27
0.3	0.49	5476	91189.12	633565.81	63.35	0.62	1.24
0.45	0.79	5476	144828.7	1006244.02	100.62	0.77	0.97
0.6	1.11	5476	203314.53	1412593.18	141.25	1.31	1.17
0.8	2.09	5476	383480.31	2664352.89	266.43	1.95	0.92

Table 3.7: Table for Chondroitin-0-Sulfate for the 8 monomer chain system showing the necessary parameters needed to find the Osmotic Pressure and showing the Standard Deviation.

3.4 Osmotic Pressure Comparison

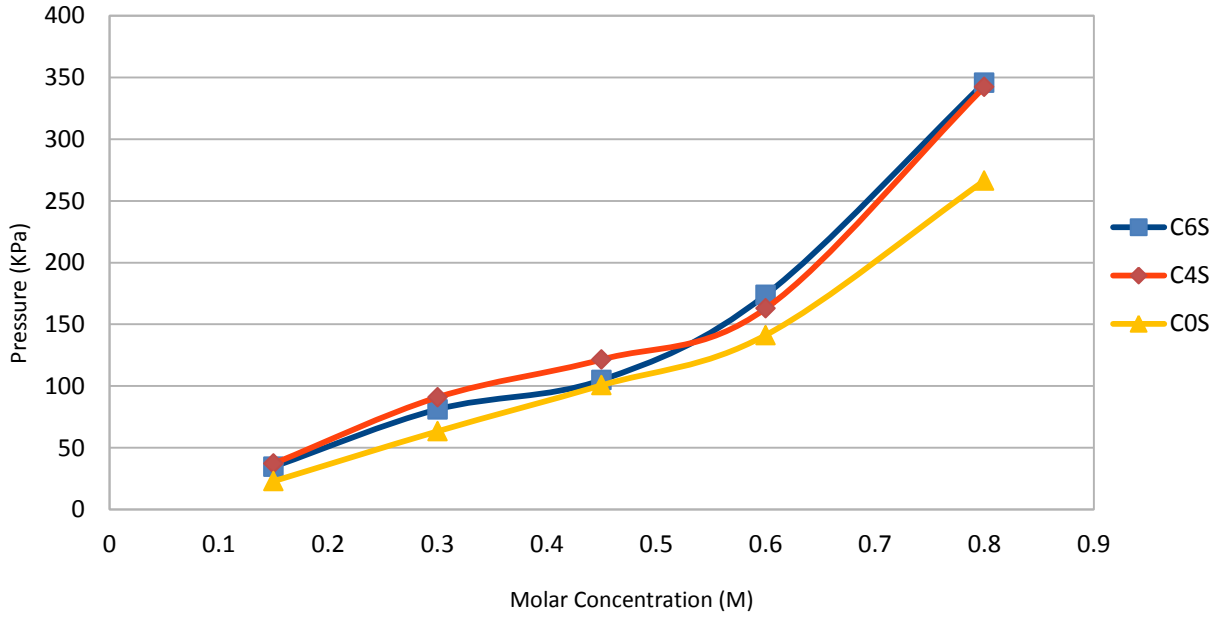

Figure 3.12: Comparison between three different CS sulfated chains (C0S, C4S, and C6S) for an 8 monomer system.

From Figure 3.12 we can see that the C4S and C6S 8 monomer chains have very similar numbers, and behave much like the 4 monomer chains. The C0S chain has slightly lower pressure values for each molar concentration, which parallels the four monomer system.

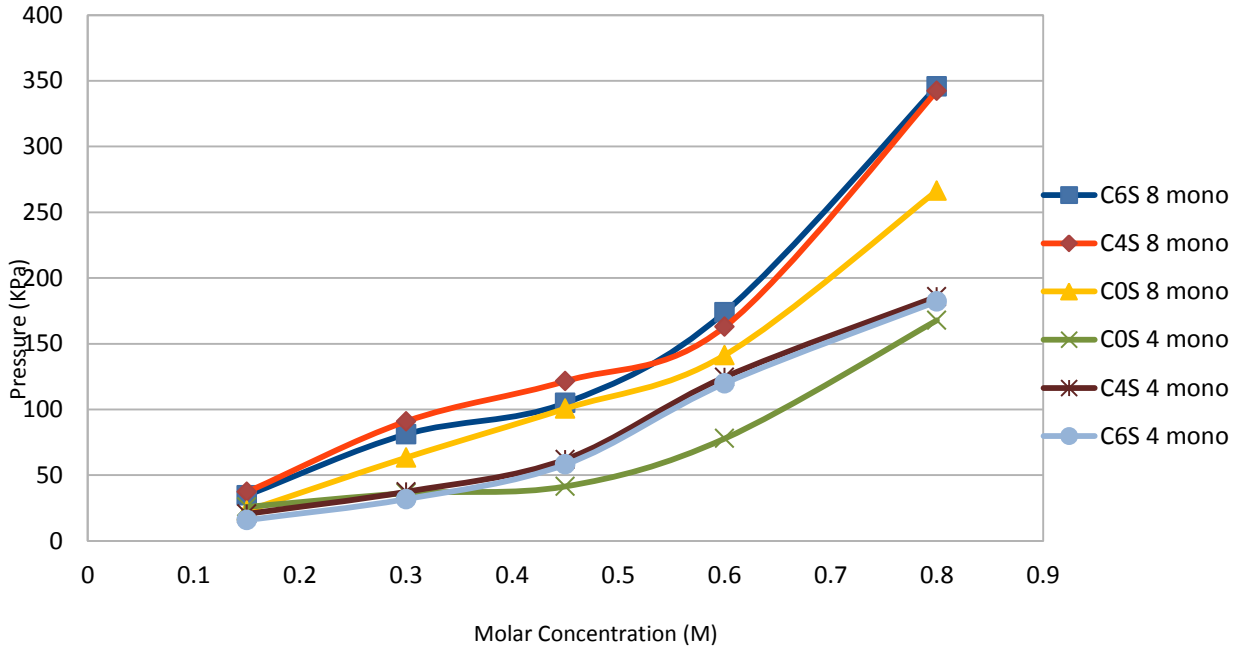

Figure 3.13: Comparison of all six chains (C0S 8 monomer, C4S 8 monomer, C6S 8 monomer, C0S 4 monomer, C4S 4 monomer, and C6S 4 monomer) in a molar concentration vs. pressure graph.

From Figure 3.13 one can interpret that the 4 monomer chain systems produce an overall less osmotic pressure than the 8 monomer systems. All of the chains are inclined upward and have a similar initial osmotic concentration. As the molar concentration increases the slope of 8 monomer chains increases as well. At .60 molar concentrations there is a further increase in pressure slope. The C6S and C4S 8 monomer chains exhibit similar behavior and have the highest pressure at .80 molar concentrations.

Chapter 4

DISCUSSION

The bulk of the experiment is aimed at figuring out what happens to GAG chains at the molecular level in articular cartilage at physiological ionic strength. CS chains are continuously subjected to compressive mechanical loading in their biomechanical environment therefore it is of primary interest to understand how changes in the chemical composition affect its mechanical properties. On that basis, an experiment was constructed to observe these force characteristics and their relationship with osmotic pressure. The system environment was replicated by building CS chains of different disaccharide lengths with different sulfation positions, and placing them in a solvation box ionized with Sodium ions. In order to replicate the experience of compression, a semipermeable membrane was built that would compress the GAG chains while leaving the water and Sodium ions to roam freely. This was imitated for different concentrations in order to account for the transient environment that articular cartilage undergoes. To this end, the experiment was designed to provide insight into the differences between CS chains based on osmotic pressure with different length and sulfation parameters. The initial validation techniques involved replicating the results attained by Roux et al. in their NaCl osmotic pressure simulation, in order to verify that our system (including configuration file, semipermeable membrane, CS chains, and solvation environment) was constructed correctly. The data followed the general trend observed in Roux et al. suggesting that the system arrangement was correct. The discrepancies are attributed to the fact that they used an NBFIX on Na+ by recalculating the R^{ij}_{min}. The tools used to conduct Luo and Roux experiments were different than that used in this study including the parameters which are revised from CHARM PARAM 27 to CHARM PARAM 36 [41].

The GAG chain system initial results using .15 M concentration gave difficult results because the force constant did not allow for enough data to be collected. Therefore a smaller force constant was inputted into the system in order to get useful results. Essentially this allows the membrane to experience the same contact with the CS chains while allowing the simulation to take more data from that contact moment. The results of this decreased force constant (.1 kcal/mol-Angstrom) correlated with the

default force constant (1 kcal/mol-Angstrom) data with a percentage error of 1.34%. This is an acceptable percentage error validating our hypothesis. This process was repeated for .30 M and .45 M with each providing percentage error of less than 1.20%.

The C4S simulations were continued using 1 kcal/mol-Angstrom as the force constant. The data showed similar results between the four sulfated and six sulfated CS chains, surmising that the sulfation position is a negligible factor in osmotic pressure determination. This is attributed to the small distance (2 Angstrom) between the position of 4- and 6- sulfation relative to the intermolecular spacing between the CS chains. The results indicate that the osmotic pressure is predominantly affected by intermolecular carboxylate-sulfate and carboxylate-carboxylate interactions.

Previous studies have tackled the subject of varying sulfation within a single chain of CS, their results combined with the data presented in this study were conclusive proof that osmotic pressure is insensitive to these variations [7, 41]. The only interactions that were affected are the sulfation to sulfation interaction which is why this study focused on this aspect. The results of this study are in qualitative agreement with the study of Bathe et al. [7], which examined the osmotic pressure of coarse grained GAG chains. The experiment conducted here, using a full atomistic model, providing a more accurate in depth gaze into the characterization of the proteoglycans. Both studies demonstrate that the osmotic pressure of the GAG system systems increase with molar concentration. However, quantitatively the measured pressures differ slightly with sulfation and disaccharide length from previous studies. These differences are attributed to the different testing methodologies by each experiment. The Bathe et al. study did not use a full atomistic model, this experiment allowed for a far more accurate description of CS chains in articular cartilage. They also utilized a different method in order to deduce the osmotic pressure. The author's results were based on an approximate molecular model that contains numerous potentially limiting assumption and theories such as the Donnan theory and the Poltzzman-Boltz cylindrical cell model. Instead this experiment utilized the method explored by Roux et. al to predict the electrostatic contribution to the osmotic pressure [41]. In our recent study mechanical loading in the form of a semipermeable membrane biaxial force in the x direction was used to estimate the osmotic pressure within cartilage.

Chondroitin Sulfate chains are composed of between 50 and 100 disaccharides. The data from the two and four disaccharide CS chains provided valuable data. For the data to be relatable to the actual physiological environmental in articular cartilage the length of the initial CS chain (2 disaccharides) was doubled and its characteristics were studied. The relationship between length and osmotic pressure can be used to analytically expand on the behavior present within a physiological environment. The

results showed that as the length of the chain was doubled, the osmotic pressure also increased at an almost parallel rate for each sulfation chain. As a result one can use this rate to predict the osmotic pressure at realistic values of 50 to a 100 disaccharides.

Another important factor that must be analyzed is the role of chain stiffness and its relationship between osmotic pressure. Past studies have conducted predictive experiments on rigid bodies; this data was compared and contrasted with the data captured in this study [7, 8]. The findings showed a slight increase from the rigid compound to the more realistic compound. This is attributed to the full atomistic model that is utilized in this experiment which provides motion and force relationships that are not taken into account in the more rigid bodies used in previous studies.

In order to optimize future developments the researchers can supplement the simulations to incorporate quantum mechanics calculations. The combination of quantum mechanics and classic mechanics would deliver more accurate results for the present work. The basic idea is to use a Quantum mechanics method for the chemically active region and use molecular mechanics treatment for the surroundings (e.g. solvent and CS chains). Accurate descriptions of the electrostatic forces on quantum mechanics subsystems due to the molecular mechanics environment, is essential for attaining a reliable modelling of biomolecules. This addition would increase computational costs exponentially but as computer technology advances, the possibilities available for processing will greatly increases. Therefore attainment of better technology would lead to more accurate results. Another advancement to this project which would lead to more precise results is the calculation of Lennard-Jones potential for each of the interactions between the atoms in the GAG chains. This is a time expensive process that would lead to increased computational expense. This option was dismissed early on in the experiment because CHARM PARAM 36 proved to have respectable data, and the time cost of calculating each Lennard Jones potential would be far too great for negligible differences in output data. As specified above the results of this experiment provided us with the framework for finding the overall osmotic pressure in realistic environments. From this point it is important to build 8 and 16 disaccharide systems and run the same simulations in order to find the rate of osmotic pressure increase. After all 4 disaccharide systems have been analyzed and an osmotic pressure mean rate has been found, it can be used to find the osmotic pressure of realistic lengths within articular cartilage.

Past studies have suggested that these macromolecules contribute far more significantly to the compressive modulus than suggested from Donnan osmotic effects alone. It was of importance to estimate the extent by which proteoglycans might contribute to the overall compressive stiffness of articular cartilage and decipher if this contribution arises from the osmotic pressure alone. This analysis

predicted that osmotic effects contribute a significant amount of the compressive modulus of cartilage, consistent with prior literature reports based on measuring properties of cartilage in isotonic and hypertonic salt solutions.

In conclusion, this study finds that the osmotic pressure of CS chains measured at physiological environments within articular cartilage increases with increase in molar concentration. The greatest slope of increase was observed in the molar concentration from .60 M to .80 M for all six chain systems. The osmotic pressure is attributed mostly to intrinsic effects, not electrostatic as previously assumed, within the articular cartilage's environment that make the osmotic pressure an increasing function of molar concentration at different ionic strengths [8]. This finding is important for several reasons, it pinpoints an important factor in compression/tension within the extracellular matrix of the articular cartilage. The negative electrostatically induced charge allows for the CS chains to act as charged rods providing energy in the compression cycle. This study provides the most up to date detailed high-order Glycosaminoglycan system model simulation in a physiological environment. Moreover, the results have shown congruency with previous simpler models, while providing significant data dissimilarities that must be further analyzed in order to more thoroughly understand the characteristics of Chondroitin Sulfate.

APPENDIX A

Tcl Scripts

I. Configuration File

```
set homeDir                .
set outputDir   .
set commonDir              .

set baseFile  ionized
# set prevJob  conc20b
set thisJob  conc20c

### run specific parameters


structure          $baseFile.psf
coordinates         $baseFile.pdb

outputName          $thisJob
XSTfile             $thisJob.xst

# set up cell size or bincoordinates and extended system

# bincoordinates      $prevJob.restart.coor
# binvelocities       $prevJob.restart.vel
# extendedSystem      $prevJob.restart.xsc

### equilibration specific parameters
useGroupPressure      yes ;# needed for 2fs steps
useFlexibleCell       no  ;# no for water box, yes for membrane
useConstantRatio      no  ;# no for water box, yes for membrane
useConstantArea               no
```

```
langevin                on
langevinTemp            295
langevinDamping         1
langevinHydrogen        off

temperature     300

# pressure control

langevinPiston          off
langevinPistonTarget    1.01325
langevinPistonTemp      295
langevinPistonDecay     100
langevinPistonPeriod    200

switching               on
switchDist              10
cutoff                  12
pairlistdist            14
margin                  3

### common parameters

binaryOutput            yes
binaryRestart           yes

parameters              par_chondroitin_all_v10.prm
paraTypeCharmm          on

if {1} {
cellBasisVector1    74 0.0 0.0
cellBasisVector2    0.0 74 0.0
cellBasisVector3    0.0 0.0 74
cellOrigin      37 37 37
}

wrapAll                 on
wrapNearest             on
wrapWater               off
```

```
COMmotion               no

outputEnergies          100
outputTiming            500
xstFreq                 500
dcdFreq                 100
restartFreq             100

timestep                2
rigidBonds                      all
nonBondedFreq           1
fullElectFrequency      4
stepsPerCycle           20

Pme                     on
PmeGridSpacing                  1

exclude                 scaled1-4
1-4scaling              1

#############################################################################

tclBC on
tclBCScript {
  set max          61.5
  set min                9.5
  set ForceConstant   1.0
  set pdbSource      ionized.pdb
  set tclBCScript    conc1.tcl
  source $tclBCScript
}
tclBCArgs { }

minimize                2000

run                             5000
```

II. Semipermeable Membrane Force

```
# we will use the following variable to calculate and print the average
# number of ions found outside the sphere at each step

set avgNumIons 0
set Salto 0

wrapmode cell

#####################################################

proc calcforces {step unique} {

 global Radius ForceConstant avgNumIons Salto max min delX

 if { $step > 0 && $step % 10000 == 0 } {

  set avgNumIons [expr $avgNumIons / 100.]
  print "Step $step, average number of ions outside the sphere: $avgNumIons"

  set avgNumIons 0

  cleardrops

 }

 set ForceStep 0
 set IonsOutside 0


                        while {[nextatom]} {


                         if { [getid] > 380 && [getid] < 38463 } { #se è acqua dimenticala
                            dropatom ;
                            incr Salto
                            continue
                          }
```

```
if { $step % 1 == 0 } {

        # vector between the ion and the sphere's center

            set rvec [getcoord]
            foreach {x y z} $rvec { break }
            set absX [expr (abs($x))]


        if { $absX < $min || $absX > $max} {
            #calcola di quanto è "fuori" lungo x rispetto  volume permesso
in modo che poi gli applico in uno step una                    #forza sufficiente a farla
rientrare
            #set delX [expr ($absX - $Radius)]
            #set deltaX [expr (abs($delX))]
            #set forceX [expr (-$ForceConstant * $deltaX)]
            if { $x < $min} {
            set delX [expr ($absX - $min)]
            set deltaX [expr (abs($delX))]
            set forceX [expr ($ForceConstant * $deltaX)]
            addforce "$forceX 0 0"
            }
            if {$x > $max} {
            set delX [expr ($absX - $max)]
            set deltaX [expr (abs($delX))]
            set forceX [expr (-$ForceConstant * $deltaX)]
            addforce "$forceX 0 0"
            }
            set ForceStep [expr ($ForceStep + abs($forceX))]
            print "Step $step          Force $forceX, Tot $ForceStep"
            incr avgNumIons
            incr IonsOutside
            #} else {
            #  dropatom ;# this ion is already inside the sphere
        }
    }
}
```

```
  # at the end of cycle over atoms print info every n steps

  if { $step % 1000 == 0 } {
                                print "Step $step          Force $ForceStep   IonsOutside $IonsOutside"
        print "atomi saltati $Salto"
  }

}
```

APPENDIX B

Molecular Dynamics Process

The molecular Dynamics process starts with input parameters that consist of particle mass, volume of the system, potential energy expression, coordinates and velocities for each particle at the initial starting point. The forces of the system are calculated using the potential energy derivative. Then Newton's laws are integrated into the process and the new coordinates and velocities are found. These steps are repeated several times in order to propagate the system through time. This allows for dynamic properties to be calculated from the MD trajectory obtained by the evolution in time of coordinates and velocities.

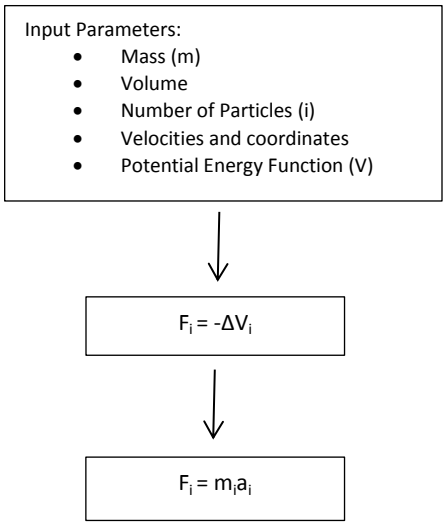

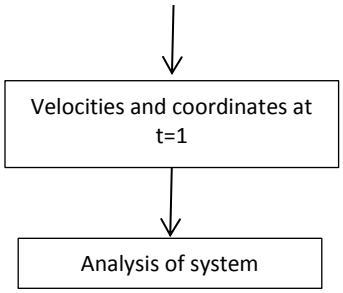

Schematic Flow Diagram of the process of the Molecular Dynamics program.

A potential energy function describes the energy of the system and it is the sum of bond terms and non-bond terms.

$$V(r) = \sum V_{bonded} + \sum V_{non-bonded}$$

The V_{bonded} term represents the interaction among bonded atoms and it is composed by bonds, angles and bond rotations terms:

$$V_{bonded} = V_{b-stretch} + V_{angle-bend} + V_{diedral-tor}$$

The first term is the bond stretching potential energy and describes the interaction between atomic pairs. It is modeled as a harmonic spring in the following equation:

$$V_{b-stretch} = \frac{1}{2} k_b (r - r_0)^2$$

Where k_b is the stiffness constant of the bond which depends on chemical type of atoms, r is the distance between atoms and r_0 is the equilibrium distance.

The second term is the potential energy of the angle bending. It is represented again by a harmonic potential where k_a is the angle stiffness, θ is the current angle and θ_0 is the optimized angle.

$$V_{angle-bend} = \frac{1}{2}k_a(\theta - \theta_0)^2$$

The third term is the torsion angle potential that describes the interaction among four atoms separated by three covalent bonds. This potential evaluates rotations by the dihedral angle f, the coefficient of symmetry n and it is assumed to be periodic.

$$V_{diedral-tor} = k_\phi(1 - \cos(n\phi))$$

The $V_{non\text{-}bonded}$ term represents the contribution of non-bonded interactions, the Van der Waals interaction energy and the Coulomb energy.

$$V_{non-bonded} = V_{VdW} + V_{Coulomb}$$

The Van der Waals potential is the balance between repulsive and attractive forces for a pair of non-charged atoms. The Lennard-Jones potential is often used as an approximate model for the isotropic part of a total (repulsion plus attraction) van der Waals' force as a function of distance.

$$V_{LJ} = 4\varepsilon\left[\left(\frac{\sigma}{r}\right)^{12} - \left(\frac{\sigma}{r}\right)^{6}\right] = \varepsilon\left[\left(\frac{r_m}{r}\right)^{12} - 2\left(\frac{r_m}{r}\right)^{6}\right],$$

where ε is the depth of the potential well, σ is the finite distance at which the inter-particle potential is zero, r is the distance between the particles, and r_m is the distance at which the potential reaches its minimum.

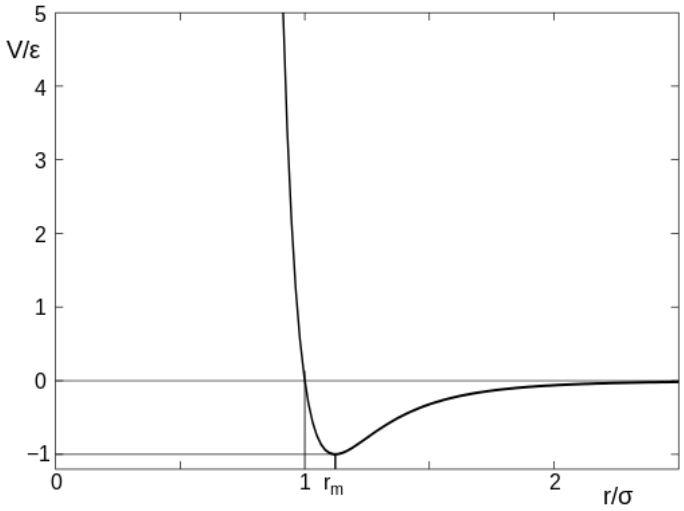

Lennard-Jones Potential: Strength versus distance.

Coulomb's law states that the electrical force between two charged objects is directly proportional to the product of the quantity of charge on the objects and inversely proportional to the square of the separation distance between the two objects. In equation form, Coulomb's law can be stated as:

$$|\mathbf{F}| = k_e \frac{|q_1 q_2|}{r^2}$$

where k_e is Coulomb's constant ($k_e = 8.987\,551\,787\,368\,1764 \times 10^9\ \mathrm{N \cdot m^2 \cdot C^{-2}}$), q_1 and q_2 are the signed magnitudes of the charges, the scalar r is the distance between the charges.

The force that acts on particle i, mass m_i and acceleration a_i is obtained from Newton's motion equation and is also given by the gradient of the Potential Energy.

$$F_i = m_i a_i$$

$$F_i = -\Delta V_i$$

Combining these two equations yields the following equation:

$$-\frac{\partial V}{\partial r_i} = m_i \frac{\partial^2 r_i}{\partial t^2}$$

This equation does not provide motion evolution trajectory and velocity of each particle. In order to get this data several integration algorithms were implemented including the Verlet algorithm and the Leap-frog algorithm. The Leap-Frog algorithm can be seen below:

$$r(t+\partial t) = r(t) + v(t+\frac{1}{2}\partial t)\partial t$$

$$v(t+\frac{1}{2}\partial t) = v(t-\frac{1}{2}\partial t) + a(t)\partial t$$

These algorithms are generated from Taylor series derivatives of expansion of position and velocity. They respect the conservation of energy and momentum principles and are computationally efficient. Velocities are explicitly calculated at time t+$\frac{1}{2}$dt and are used to obtain positions at time t+dt, therefore positions and velocity are not calculated at the same time. In order to evaluate velocities at time t+dt the average between v(t- $\frac{1}{2}$dt) and v(t+$\frac{1}{2}$dt) is calculated.

Bibliography

[1] Abrikosov A.A, Gorkov L.P, Dzyaloshinsky I.E. *Methods of Quantum Field Theory in Statistical Physics.* Chapter 6 Electromagnetic Radiation in an Absorbing Medium. Dover Publications. ISBN 0-486-63228-8.

[2] Altis A, Nguyen PH, Hegger R, Stock G (2007) Dihedral angle principal component analysis of molecular dynamics simulations. J Chem Phys 126: 244111.doi:10.1063/1.2746330.

[3] "Articular Cartilage Extracellular Matrix". Glycobiology.2012 R and D system Web. 31 May. 2014. <http://www.rndsystems.com/Pathway.aspx?p=16046&r=15435>.

[4] Ateshian, G. A., N. O. Chahine, I. M. Basalo, and C. T. Hung. 2004. The correspondence between equilibriumbiphasic and triphasic material properties in mixture models of articular cartilage. J. Biomech. 37:391–400.

[5] Basser, P. J., R. Schneiderman, R. A. Bank, E. Wachtel, and A. Maroudas. 1998. Mechanical properties of the collagen network in human articular cartilage as measured by osmotic stress technique. Arch. Biochem. Biophys. 351:207–219.

[6] Batchelor, G. K. , "The effect of Brownian motion on the bulk stress in a suspension of spherical particles," J. Fluid Mech. 83, 97–117 (1977).

[7] Bathe M, Rutledge GC, Grodzinsky A, Tidor B. Osmotic pressure of aqueous chondroitin sulfate solution: a molecular modeling investigation. Biophys. J. 2005;89:2357–2371.

[8] Bathe M., Rutledge G.C., Tidor B. A coarse-grained molecular model for glycosaminoglycans: application to chondroitin, chondroitin sulfate, and hyaluronic acid. Biophys. J. 2005;88:3870–3887.

[9] Benedict M. Sattelle, Javad Shakeri, Ian S. Roberts, Andrew Almond Carbohydr Res. 2010. A 3D-structural model of unsulfated chondroitin from high-field NMR: 4-sulfation has little effect on backbone conformation. January 26; 345(2): 291–302. doi: 10.1016/j.carres.2009.11.013

[10] Brooks BR, Brooks CL, III, Mackerell AD, Jr., et al. CHARMM: the biomolecular simulation program. *Journal of Computational Chemistry*. 2009;30(10):1545–1614.

[11] Buckwalter JA, Hunzinker E, Rosenberg L, et al. Articular cartilage: composition and structure. In: Woo SLY, Buckwalter JA, editors. , eds. Injury and Repair of the Musculoskeletal Soft Tissues. Park Ridge, IL: American Academy of Orthopaedic Surgeons; 1988:405-425.

[12] Buckwalter JA, Mow VC, Ratcliffe A. Restoration of injured or degenerated articular cartilage. J Am Acad Orthop Surg. 1994;2:192-201

[13] Canal Guterl, C., Hung, C. T., and Ateshian, G. A., 2010, "Electrostatic and Non-Electrostatic Contributions of Proteoglycans to the Compressive Equilibrium Modulus of Bovine Articular Cartilage," J. Biomech., 43(7), pp. 1343–1350.

[14] Chen FH, Rousche KT, Tuan RS. Technology insight: adult stem cells in cartilage regeneration and tissue engineering. Nat Clin Pract Rheumatol. 2006;2:373-382.

[15] "Chondroitin Sulfate Disaccharide" Prithason at en.wikipedia. 2006-03-09 http://commons.wikimedia.org/wiki/File:Chondroitin_Sulfate_Structure_NTP.png

[16] Cleland, R. L. 1971. Ionic polysaccharides. V. Conformational studies of hyaluronic acid, cellulose, and laminaran. Biopolymers. 10:1925–1948. 49. von Gru¨nberg, H. H., R. van Roij, and G. Klein. 2001. Gas-liquid phase coexistence in colloidal suspensions? Europhys. Lett. 55:580–586.

[17] Clipa G. et al (2010) Atomistic Insight into Chondroitin-6-Sulfate Glycosaminoglycans Chain Through Quantum Mechanics Calculations and Molecular Dynamics Simulation, JCC 31, 1670-1680.

[18] Ehrlich, S., N. Wolff, R. Schneiderman, A. Maroudas, K. H. Parker, and C. P. Winlove. 1998. The osmotic pressure of chondroitin sulphate solutions: experimental measurements and theoretical analysis. Biorheology.35:383–397.

[19] Ehrlich S, Wolff N, Schneiderman R, Maroudas A, Parker KH, Winlove CP. The osmotic pressure of chondroitin sulphate solutions: experimental measurements and theoretical analysis. Biorheology. 1998 Nov-Dec;35(6):383-97.

[20] Felisbino SL[1], Carvalho HF. The epiphyseal cartilage and growth of long bones in Rana catesbeiana. Tissue Cell. 1999 Jun;31(3):301-7.

[21] Feynman, Richard P. (2011). "Work and potential energy". *The Feynman Lectures on Physics, Vol. I*. Basic Books. p. 13. ISBN 978-0-465-02493-3.

[22] Forster H, Fisher J. The influence of loading time and lubricant on the friction of articular cartilage. Proc. Inst. Mech. Eng. H. 1996; 210:109–119.

[23] Frederix PL[1], Bosshart PD, Engel A. Atomic force microscopy of biological membranes. Biophys J. 2009 Jan;96(2):329-38. doi: 10.1016/j.bpj.2008.09.046.

[24] Fuentes G, Nederveen AJ, Kaptein R, Boelens R, Bonvin AM. J Biomol NMR. Describing partially unfolded states of proteins from sparse NMR data. 2005 Nov;33(3):175-86.

[25] Fung YC. Biomechanics: Mechanical Properties of Living Tissues. 2nd ed. New York (NY): Springer-Verlag; 1993.

[26] Gold LS, Manley NB, Slone TH, Ward JM. Compendium of chemical carcinogens by target organ: results of chronic bioassays in rats, mice, hamsters, dogs, and monkeys. Toxicol Pathol. 2001;29:639–652.

[27] Grodzinsky AJ, Roth V, Myers E, Grossman WD, Mow VC. The significance of electromechanical
and osmotic forces in the nonequilibrium swelling behavior of articular cartilage in tension. J. Biomech. Eng. 1981; 103:221–231.

[28] Han L, Dean D, Mao P, Ortiz C, Grodzinsky AJ. Nanoscale shear deformation mechanisms of opposing cartilage aggrecan macromolecules. Biophys. J. 2007b;93:L23–L25.

[29] Han L, Grodzinsky A, and Ortiz1 C. Nanomechanics of the Cartilage Extracellular Matrix. Annu Rev Mater Res. 2011 Jul 1;41:133-168.

[30] Hardingham TE, Muir H. The specific interaction of hyaluronic acid with cartilage proteoglycans. Biochim. Biophys. Acta. 1972; 279:401–405.

[31] Hardingham TE. Proteoglycans: their structure, interactions and molecular organization in cartilage. Biochem Soc Trans. 1981;9: 489–97.

[32] Hudson R. M., Allis G. D., Hudson S. B. The journal of Physical Chemistry. ACS Publications, November 25th, 2010. Volume 114. Number 46.

[33] Hummer, G, Kevrekidis, I. Coarse molecular dynamics of a peptide fragment: Free energy, kinetics, and long-time dynamics computations. *Journal of Chemical Physics*, 118(23):10762 - 10773, Jun 15 2003.

[34] Humphrey W, Dalke A, Schulten K (1996) VMD - Visual Molecular Dynamics. J Molec Graphics 14: 33–38.

[35] Jones LL[1], Margolis RU, Tuszynski MH. The chondroitin sulfate proteoglycans neurocan, brevican, phosphacan, and versican are differentially regulated following spinal cord injury. Exp Neurol. 2003 Aug;182(2):399-411.

[36] Kiani C, Chen L, Wu YJ, Yee AJ, Yang BB (March 2002). Structure and function of aggrecan. *Cell Res.* 12 (1): 19–32. doi:10.1038/sj.cr.7290106. PMID 11942407.

[37] Kieseritzky G, Knapp EW. J Comput Chem. Improved pK(a) prediction: combining empirical and semimicroscopic methods. 2008 Nov 30;29(15):2575-81. doi: 10.1002/jcc.20999.

[38] Kr. A. D. mackerel and al., An all atom empirical energy function for the simulation of nucleic acids, J Am. Chem. Soc 117 (1995), 11946 11975.

[39] Lauder, R. M., T. N. Huckerby, and I. A. Nieduszynski. 2000. A fingerprinting method for chondroitin/dermatan sulfate and hyaluronan oligosaccharides. Glycobiology. 10:393–401.

[40] Le Roy, Robert J.; R. D. E. Henderson (2007). "A new potential function form incorporating extended long-range behaviour: application to ground-state Ca_2". *Molecular Physics* 105 (5–7): 663. Bibcode:2007MolPh.105..663L. doi:10.1080/00268970701241656.

[41] Luo, Y.; A. D.; Roux, B. Simulation of Osmotic Pressure in Concentrated Aqueous Salt Solutions. Faraday Discuss. 2013, 160, 135– 149

[42] Maroudas A. Physiochemical properties of articular cartilage. In: Freeman MAR, editor. , ed. Adult Articular Cartilage. Kent, United Kingdom: Cambridge University Press; 1979:215-290.

[43] Mow VC, Holmes MH, Lai WM. Fluid transport and mechanical properties of articular cartilage: a review. J Biomech. 1984;17:377-394.

[44] Murad, S. A Computer Simulation of the Classic Experiment on Osmosis and Osmotic Pressure. J. Chem. Phys. 1993, 99,
7271–7271.

[45] Murad, S.; Powles, J. G.; Holtz, B. Osmosis and Reverse Osmosis in Solutions: Monte Carlo Simulations and van der Waals One-Fuild Theory. Mol. Phys. 1995, 86, 1473–1483.

[46] Murata K, Bjelle AO. Age-dependent constitution of chondroitin sulfate isomers in cartilage proteoglycans under associative conditions. J Biochem. 1979 Aug;86(2):371–376.

[47] Nap RJ, Szleifer I (November 2008). "Structure and interactions of aggrecans: statistical thermodynamic approach". *Biophys. J.* 95 (10): 4570–83. doi:10.1529/biophysj.108.133801. PMC 2576360. PMID 18689463.

[48] Narmoneva, D. A., J. Y. Wang, and L. A. Setton. 1999. Nonuniform swelling-induced residual strains in articular cartilage. J. Biomech. 32:401–408.

[49] Nielson, Kevin D.; van Duin, Adri C. T.; Oxgaard, Jonas; Deng, Wei-Qiao; Goddard, William A. (2005). "Development of the ReaxFF Reactive Force Field for Describing Transition Metal Catalyzed Reactions, with Application to the Initial Stages of the Catalytic Formation of Carbon Nanotubes". *The Journal of Physical Chemistry A* 109 (3): 493–499. doi:10.1021/jp046244d. PMID 16833370.

[50] Nordin M, Frankel VH. Basic Biomechanics of the Musculoskeletal System. 3rd ed. New York, NY: Lippincott Williams & Wilkins; 2001.

[51] Northrop JH[1], Kunitz M.J. The Swelling and Osmotic Pressure in Salt Solutions. Gen Physiol. 1926 Apr 20;8(4):317-37

[52] "Osmosis". *Encyclopaedia Britannica. Encyclopaedia Britannica Online*. Encyclopædia Britannica Inc., 2014. Web. 03 Jun. 2014. <http://www.britannica.com/EBchecked/topic/434057/osmosis>.

[53] Phillips, J. C.; Braun, R.; Wang, W.; Gumbart, J.; Tajkhorshid, E.; Villa, E.; Chipot, C.; Skeel, R. D.; Kalé, L.; Schulten, K. *J. NAMD Tutorial.* 2005, *26* (16), 1781.

[54] Phillips, J. C.; Braun, R.; Wang, W.; Gumbart, J.; Tajkhorshid, E.; Villa, E.; Chipot, C.; Skeel, R. D.; Kalé, L.; Schulten, K. *J. NAMD tutorial: User-Defined Forces.* 2005, *26* (16), 1781.

[55] Plimpton SJ. Fast parallel algorithms for short-range molecular dynamics. J. Chem. Phys. 1995;117:1–19.

[56] Robinson CR, Sligar SG. Hydrostatic and osmotic pressure as tools to study macromolecular recognition. Methods Enzymol. 1995;259:395-427.

[57] Roughley P. J., Lee E. R. 1994. Cartilage proteoglycans: structure and potential functions. *Microsc. Res. Tech.* 28: 385–397 doi: 10.1002/jemt.1070280505.

[58] Schaefer P, Riccardi D, Cui Q. Reliable treatment of electrostatics in combined qm/mm simulation of macro-molecules. Journal of Chemical Physics. 2005 Jul;123(1):014905.

[59] Seog J., Dean D., Ortiz C. Direct measurement of glycosaminoglycan intermolecular interactions via high-resolution force spectroscopy. Macromolecules. 2002;35:5601–5615.

[60] Shengyi, T., and Xu, Y., 1991, "Biomechanical Properties and Collagen Fiber Orientation of TMJ Discs in Dogs: Part 1. Gross Anatomy and Collagen Fiber Orientation of the Discs," J. Craniomandib. Disord., 5, pp. 28–34.

[61] Tria J.A., "The Knee: A Comprehensive Review" World Scientific, 2010. 9814282049, 9789814282048.

[62] Uesaka S[1], Miyazaki K, Ito H. Age-related changes and sex differences in chondroitin sulfate isomers and hyaluronic acid in normal synovial fluid. 2004 Dec;14(6):470-5. doi: 10.3109/s10165-004-0351-0.

[63] Van de Velde SK, Bingham JT, Hosseini A, Kozanek M, DeFrate LE, et al. Increased tibiofemoral cartilage contact deformation in patients with anterior cruciate ligament deficiency. Arthritis Rheum. 2009; 60:3693–3702.

[64] Watanabe H[1], Yamada Y, Kimata K.Roles of aggrecan, a large chondroitin sulfate proteoglycan, in cartilage structure and function.

[65] "What is cartilage made of?" Joint Specialists of W.N.C., 2014 Web 18 May. 2014. http://www.hendersonvilleorthopedics.com/faq/what-is-cartilage-made-of/.

[66] Winter DA. Biomechanics and Motor Control of Human Movement. Second. New York: A Wiley-Interscience Publication; 1990.